MTP-AERO-62-76
October 22, 1962

GEORGE C. MARSHALL SPACE FLIGHT CENTER

HUNTSVILLE, ALABAMA

A METHOD OF DETERMINING THE SOURCE OF ERRORS IN GUIDANCE MEASUREMENTS AND THE RESULTANT ERRORS IN EARTH-FIXED COMPONENTS

By

R. A. Chapman

NASA

FOR INTERNAL USE ONLY

GEORGE C. MARSHALL SPACE FLIGHT CENTER

MTP-AERO-62-76

A METHOD OF DETERMINING THE SOURCE OF ERRORS IN GUIDANCE MEASUREMENTS AND THE RESULTANT ERRORS IN EARTH-FIXED COMPONENTS

R. A. Chapman

ABSTRACT

This report presents a method for determining sources of error in inertial guidance system measurements.

Analysis of a two-stage, 555-kilometer Saturn orbit revealed typical profiles for the first stage and total flight. Guidance errors are presented in terms of earth-fixed trajectory components at the time of first stage cutoff and injection parameters at second stage cutoff.

A least squares method is used to determine sources of guidance intelligence errors.

The method presented in this report indicates that error sources apparently insignificant or unmeasurable during the first stage become quite significant during the longer acceleration time inherent to the second stage.

GEORGE C. MARSHALL SPACE FLIGHT CENTER

MTP-AERO-62-76

October 22, 1962

A METHOD OF DETERMINING THE SOURCE OF ERRORS IN GUIDANCE MEASUREMENTS AND THE RESULTANT ERRORS IN EARTH-FIXED COMPONENTS

by
R. A. Chapman

FLIGHT EVALUATION BRANCH
AEROBALLISTICS DIVISION

TABLE OF CONTENTS

LIST OF FIGURES

LIST OF FIGURES (CONT.)

LIST OF TABLES

DEFINITION OF SYMBOLS

Symbol	Parameter
X, Y, Z	Space-fixed axes of the stabilized platform
X_m, Y_m, Z_m	Inertial measurements along platform axes
X_e, Y_e, Z_e	Earth-fixed plumbline coordinates origin at launch site
X_e', Y_e', Z_e'	Earth-fixed ephemeris coordinates origin at center of earth
ξ, η, ζ	Inertial guidance coordinates
ξ_i, η_i, ζ_i	Guidance indications including preset and programmed values
$\Delta\dot{\xi}, \Delta\dot{\eta}, \Delta\dot{\zeta}$	Ideal minus variation guidance velocity differences
$\Delta X_e, \Delta Y_e, \Delta Z_e$	Ideal minus variation plumbline coordinate differences
ΔR	Error in Radial distance from center of earth to vehicle
ΔV_e	Error in earth-fixed velocity
$\Delta\epsilon_v$	Error in local elevation angle of velocity vector
$\Delta\alpha$	Error in local azimuth of velocity vector
$\Delta\psi$	Error in geocentric latitude
$\Delta\lambda$	Error in longitude

GEORGE C. MARSHALL SPACE FLIGHT CENTER

MTP-AERO-62-76

A METHOD OF DETERMINING THE SOURCE OF ERRORS IN GUIDANCE MEASUREMENTS AND THE RESULTANT ERRORS IN EARTH-FIXED COMPONENTS

By R. A. Chapman

SUMMARY

This report presents a method of evaluating an all-inertial guidance system utilizing integrating accelerometers and air-bearing gyros for stabilization of the reference element. The errors in the guidance measurements are placed in two general classes, functional errors and guidance intelligence errors. Functional errors are those that may be generally determined from the telemetered data; the guidance intelligence errors are those that result from accelerometer errors and any instantaneous misalignment of the reference element.

The sources of guidance intelligence errors may be determined by a least squares method. The inputs to the program are: (1) residuals obtained from a comparison of the telemetered guidance measurements with a reference trajectory and (2) partial derivatives obtained from perturbed standard trajectories.

The significant errors to be expected in cross range measurements would result from initial misalignment of the reference element and/or "g"-dependent drifts of the stabilizing gyros. The more significant errors in slant range and slant altitude measurements would result from accelerometer scale factor errors.

A standard or ideal trajectory was calculated for a two-stage, 555-km orbital mission of a Saturn vehicle. This ideal trajectory was perturbed to determine the effects of the guidance errors. Guidance was in "open loop" for the trajectory calculations so that flight event

times were identical. However, the differences between the perturbed and ideal values represent the true guidance intelligence errors.

Guidance system hardware errors (1σ) introduced produced additive effects on the accelerometer outputs. This represents the maximum possible intelligence error that could occur from one sigma error sources. The resultant intelligence errors at second stage cutoff in terms of earth-fixed positions and velocities are:

$$\Delta X_e = \mp 1009 \text{ m} ; \qquad \Delta \dot{X}_e = \mp 1.5 \text{ m/s}$$

$$\Delta Y_e = \pm 679 \text{ m} ; \qquad \Delta \dot{Y}_e = \pm 3.1 \text{ m/s}$$

$$\Delta Z_e = \pm 1405 \text{ m} ; \qquad \Delta \dot{Z}_e = \pm 3.6 \text{ m/s}$$

and in terms of injection parameters:

$$\Delta R = \pm 422 \text{ m} ; \qquad \Delta \alpha_v = \pm 0.023 \text{ deg}$$

$$\Delta V_e = \mp 2.1 \text{ m/s} ; \qquad \Delta \psi = \mp 0.010 \text{ deg}$$

$$\Delta \epsilon_v = \pm 0.012 \text{ deg} ; \qquad \Delta \lambda = \mp 0.012 \text{ deg}$$

INTRODUCTION

Guidance is necessary in order to steer a vehicle into a predetermined set of conditions to rendezvous with a prescribed target. It was assumed for the studies that the guidance system was an all-inertial system completely independent of ground or radio control after liftoff. However, some provision may be made to adjust, during flight, the constants in the guidance equations stored in the onboard guidance computer.

This report discusses the analysis of guidance errors resulting from: (1) initial misalignments of both the accelerometers and stabilizing gyros, (2) drift of the stabilized element during flight, and (3) errors in measuring the vehicle motions. Also, the resultant effects of these guidance errors on the set of conditions required to accomplish a particular mission are presented.

The computations were for a two-stage Saturn C-1 vehicle with a mission to put a payload into a 555-km orbit. Trajectory computations considered guidance in "open loop" so that flight event times were identical. However, the differences between perturbed and ideal outputs represent the guidance intelligence errors. Hardware alignments assumed for the trajectory computations were those to be used throughout the Block I Saturn vehicles and a portion of the Block II vehicles.

The guidance system during flight must obtain information as to local state (time, thrust acceleration, position, and velocity), make a decision based on this information as to how the vehicle should be steered, carry out the required maneuvers, and terminate thrust at the proper instant. The "delta minimum" guidance mode does this by comparing the measured values with those on a precalculated "standard" trajectory which will cause the fulfillment of the mission if followed. The nulling of the differences in the variables is then the basis of steering commands for the vehicle.

A guidance system utilizing the "Path-Adaptive" mode measures the state variables at the initial point and solves a set of differential equations for parameters that will steer the vehicle along an optimum trajectory so that the variables satisfy the mission equations at the terminal point. The solution provides a set of time functions that represent the optimum trajectory based on no future disturbances. However, as soon as some disturbance occurs a new set of functions is called for. The "Path-Adaptive" mode does not constrain the flight to a prescribed path. Instead, an optimum trajectory is determined, based on measured values, and steering commands are generated to steer the vehicle along the selected trajectory.

Complete "closed loop" guidance will probably be used only in upper stages in Saturn flights. However, measurements will be made during the first flight stage to furnish initial values for closed loop computations.

Accelerometers mounted on the stabilized element sense the vehicle motions along a set of mutually perpendicular, space-fixed axes. Outputs of the accelerometers are time integrals of the vehicle motions or inertial velocity measurements. These velocities are processed, telemetered, and fed into the guidance computer. The computer outputs are processed and the appropriate signals are fed into the control computer and system network. Necessary signals to align the vehicle according to the steering commands are generated in the control computer. Truncations of the guidance equations may permit small dispersions to be undetected and hence uncorrected. Abnormal disturbances, such as fuel depletion before the necessary cutoff conditions are attained, are sensed by the guidance system, but the resulting dispersions may not be corrected.

The outputs of the guidance computer monitored on the ground can be analyzed for flight adjustments and guidance errors. Corrections may be obtained and transmitted to the vehicle during a coast phase to be executed by the guidance system during a later burning stage. However, a complete evaluation of the guidance system requires more time than would be permitted for a relatively short coast period.

The guidance measurements furnish continuous "tracking data" from onboard the vehicle and may be utilized to establish a complete trajectory or to cover flight periods where ground tracking is either unavailable or unreliable. However, a method of determining the gravitational components from the inertial guidance measurements is required. Once the gravitational components are determined the inertial measurements then may be directly converted into earth-fixed tracking data.

1.0 INERTIAL GUIDANCE SYSTEM DESCRIPTION

A completely inertial guidance system employs gyroscopic accelerometers which convert acceleration signals into velocity information. This velocity data is used in the guidance computers to produce displacement or position data. All guidance intelligence is contained or generated within the vehicle and is independent of outside sources during flight.

The guidance system consists of a gyro-stabilized platform, three integrating accelerometers mounted on the stable platform, guidance computers, a program device, and associated power supply and electrical circuitry.

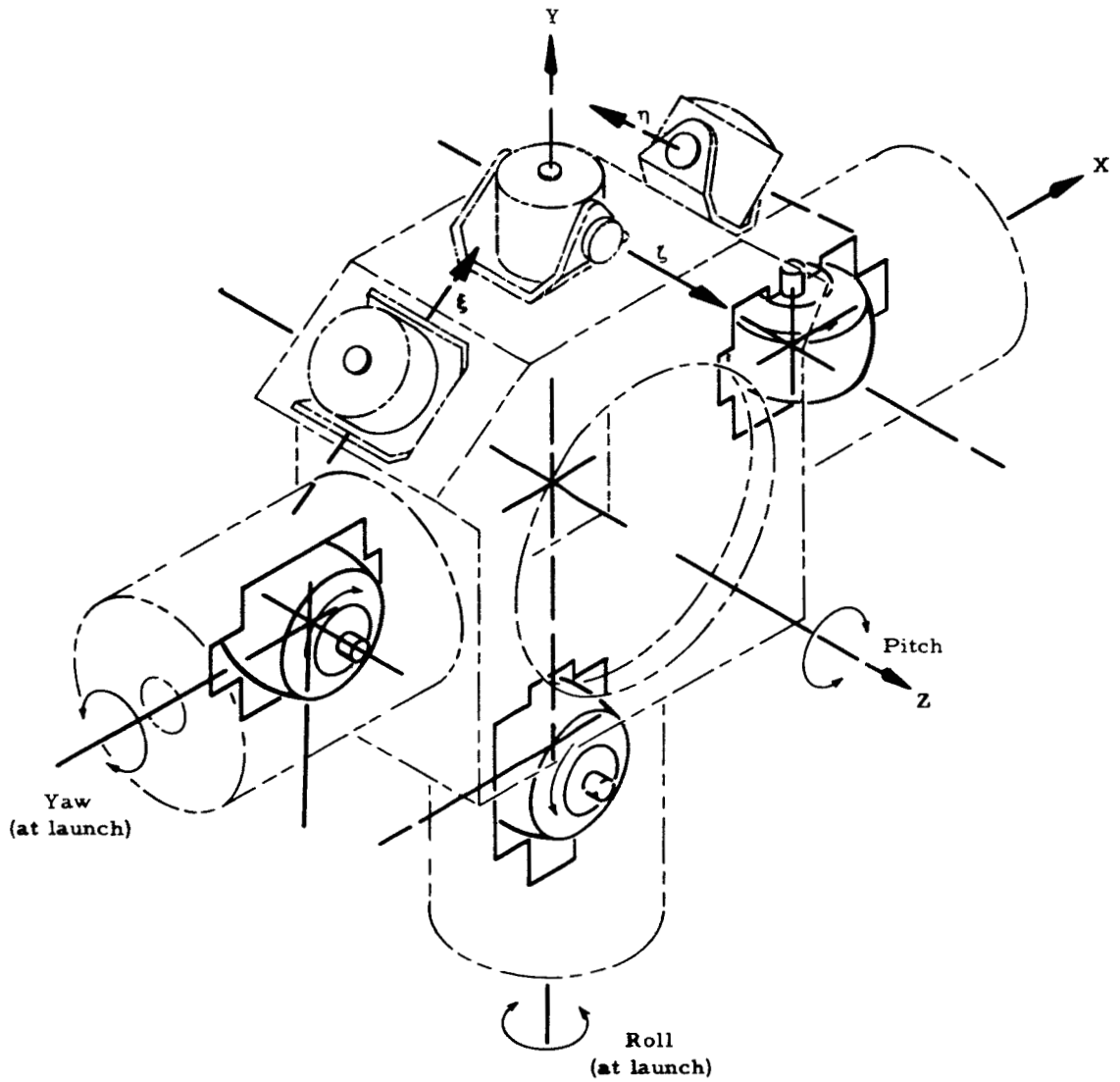

MTP-AERO-62-76

FIG. 1. RELATIONSHIP OF PLATFORM, TRANSLATIONAL, AND STABILIZING AXES

The platform is gyro-stabilized along three mutually perpendicular axes as shown in Figure 1. The space-fixed orientation at the instant of launch is maintained throughout the controlled flight. The axes are in a right-handed Cartesian coordinate system with the X- and Z-axes lying, at the instant of launch, in the plane tangent to the earth at the launch site. The positive X-axis lies along the firing azimuth. The Y-axis is normal to the tangent plane at the point of tangency with the positive direction upward along the local plumbline at the instant of launch.

The accelerometers are mounted on the stable platform oriented along three mutually perpendicular translational measuring axes ξ, η, and ζ. Inertial measurements are made in the slant range, slant altitude, and cross-range directions. The positive ξ axis lies in the platform XY plane, the positive η axis is normal to the ξ axis in the platform XY plane, and the positive ζ axis is normal to the $\xi\,\eta$ plane and parallel to the platform Z axis. This coordinate system is space-oriented at the instant of launch and remains fixed throughout the controlled flight. The fixed relationship between the coordinate axes of the stabilized platform and the translational measuring axes is shown in Figure 1.

Three mutally perpendicular rotational measuring axes are fixed to the stabilized platform. They are the axes about which the vehicle air frame rotates relative to the platform carrier ring. Free to rotate in these directions, the gimbal system isolates the platform carrier ring from the rotational motion of the vehicle air frame. The gimbal axes are pitch, roll, and yaw. Under ideal conditions with no roll or yaw vehicle attitude errors, the pitch axis is parallel to the cross-range direction. The roll axis is parallel to the vehicle longitudinal axis at launch. Measurements made around these axes are concerned with vehicle attitude and thus are data to be used in the control computer. These measurements do not affect the guidance intelligence unless they exceed specified rotational limits thus forcing the stabilized platform out of its frame of reference. The Saturn (ST-124) platform to be used in closed loop has unlimited gimbal freedom about three axes provided by a four-gimbal configuration. This will eliminate the possibility of gimbal lock. A schematic of Saturn inertial platform is shown in Figure 2.

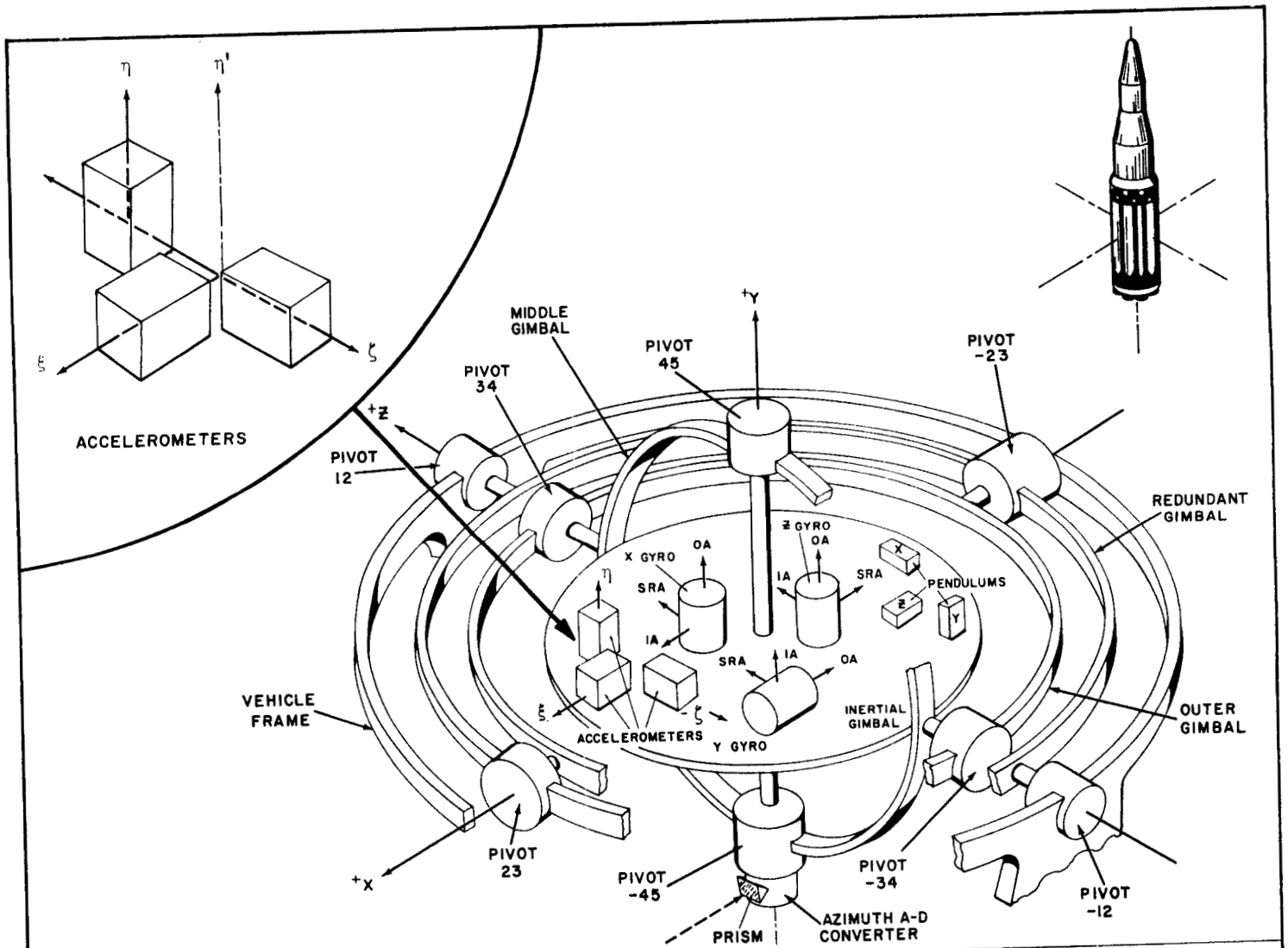

MTP-AERO-62-76

FIG. 2. SATURN PLATFORM SCHEMATIC

The relationship of the rotational axes to the stabilized platform and the translational measuring axes is shown in Figure 1. In addition to these three coordinate systems each individual stabilizing gyro and gyroscopic accelerometer contains a set of axes. These axes are shown for the stabilizing gyros only but similar ones apply for the accelerometers. The gyro axes are referred to as spin, output or precession, and input axes.

A simplified diagram of the Saturn Guidance and Control System is shown in Figure 3. The system consists principally of three major sub-systems: (1) a four-gimbal inertial platform with three orthogonal accelerometers mounted on the stable element and attitude resolvers on each gimbal; (2) a general purpose digital guidance computer; and (3) an analog control computer with associated sensors and actuators. Interface requirements between these sub-systems are provided in the guidance signal processor.

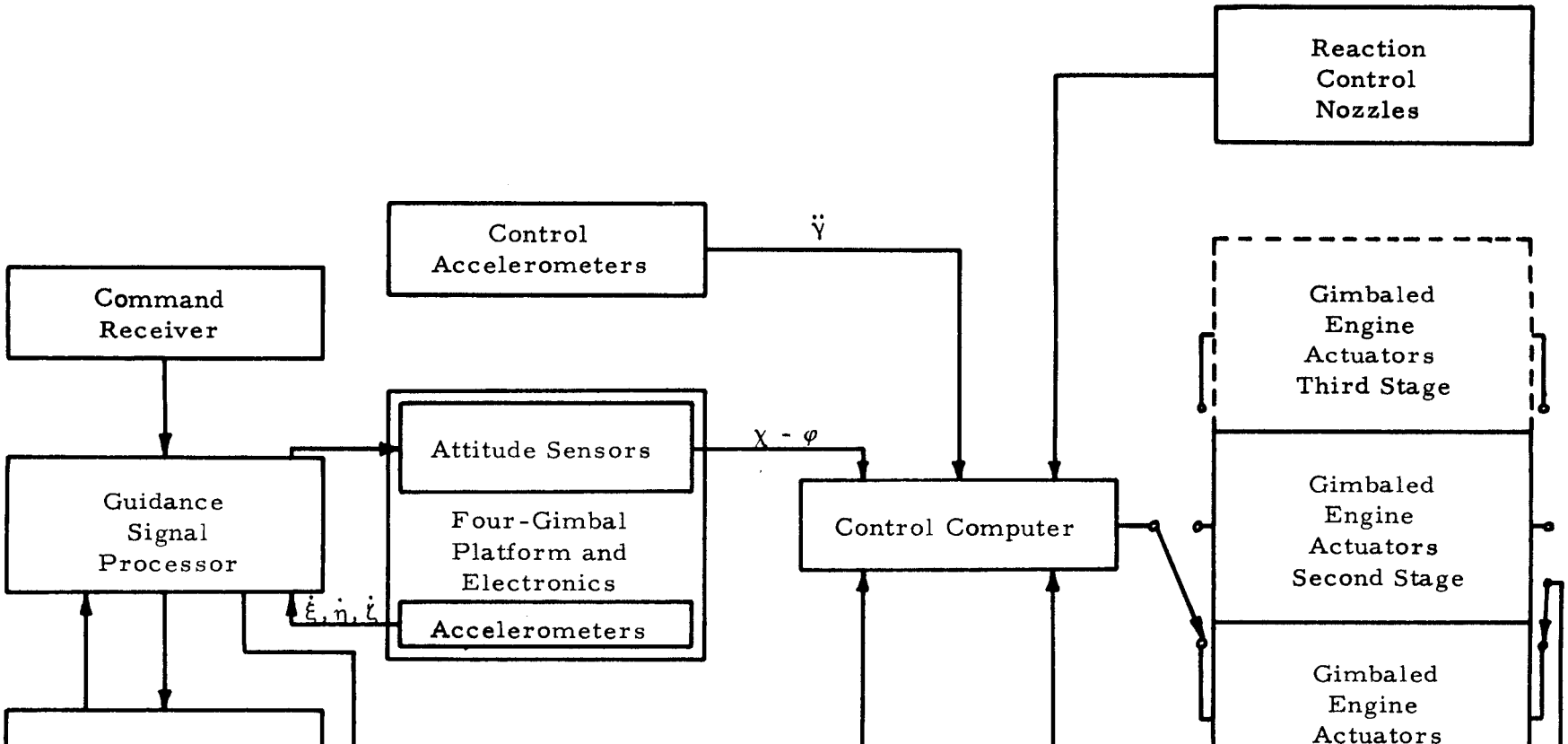

MTP-AERO-62-76

FIG. 3. SATURN GUIDANCE AND CONTROL SYSTEM

2.0 SOURCES OF GUIDANCE DATA

Vehicle flight data used for evaluating an inertial guidance system consists of two basic types: (1) onboard measurements and monitoring signals including the actual outputs of the guidance computers and (2) earth-fixed positions determined from electronic and/or optical tracking independent of the guidance system.

2.1 Telemetry

The telemetered data used to evaluate the performance of the guidance system may be grouped in three classes: (1) inertial displacements and velocity measurements, (2) functional monitoring signals, and (3) indirect guidance measurements.

2.1.1 Displacement and Velocity Measurements

The motions of the vehicle along the translational measuring axes are sensed by the integrating accelerometers and integrated onboard the vehicle into position data. During the first stage of flight these data are stored for computations to be performed during the second burning stage.

The guidance and control system is designed to control the vehicle along an optimum flight path and to terminate thrust at the proper instant. The vehicle is guided along one of an array of trajectories that will satisfy conditions required to accomplish the mission of the payload.

2.1.2 Functional Monitoring

Direct monitoring of the various components during flight furnishes data indicating the functional performance of the guidance system. Table I lists some typical monitoring measurements.

TABLE I

TYPICAL MONITORING MEASUREMENTS

1.	Servo Error Signals	Guidance Accelerometers
2.	Servo Error Signals	Guidance Computers
3.	Pulses from Program Device	Network Commands

The servo-error signals represent frictional torques, or lags in the system network, which are continuously compensated for or corrected by the associated servo system. An examination of the error-signal measurements will give an indication of the effects of vibrations and other flight disturbances on the guidance measurements.

Pulses from the program device represent the times of flight at which programmed network commands are executed. These times should be identical with those of the standard program. A predetermined "time of events" is put on a magnetic tape and stored in the program device. Examples of the programmed commands are:

1. Control gain factors entered or changed in the control computer
2. First stage tilt start and end
3. End first stage thrust (IECO + Δt)
4. Separation of stages
5. Activate guidance steering commands

2.1.3 Indirect Guidance Measurements

Supporting measurements pertaining to guidance are the angular rotations of the vehicle with respect to the stabilized platform and the angular deflections of the thrust vector. Typical supporting measurements are listed in Table II.

TABLE II

SUPPORTING MEASUREMENTS FOR GUIDANCE ANALYSIS

	Measurement	Symbol	
1.	Platform position pitch	φ_p	deg
	a. Programmed tilt angle	χ	deg
	b. Pitch difference angle	$\Delta\varphi_p$	deg
2.	Platform position yaw	φ_y	deg
3.	Platform position roll	φ_r	deg
4.	Vehicle angular rate	$\dot{\varphi}_p$, $\dot{\varphi}_y$, $\dot{\varphi}_r$	deg/sec
5.	Angle of attack pitch	α_p	deg
6.	Angle of attack yaw	α_y	deg
7.	Engine deflection angle pitch	β_p	deg
8.	Engine deflection angle yaw	β_y	deg
9.	Engine deflection angle roll	β_r	deg
10.	Voltage level	Power supply	

The measurements 1.b through 6 in Table II are essentially control parameters used in the control computer to generate signals for attitude control. This program tends to control the vehicle attitude and prevent excessive drifts due to winds. By introducing the computed steering commands into the control computer, correction signals are generated to align the vehicle with the instantaneous optimum trajectory. The correction signals generated in the control computer initiate deflections of the thrust vector thus guiding the vehicle along a selected trajectory until cutoff conditions are fulfilled.

Errors made on these measurements have an indirect effect on the performance of the guidance system in that the vehicle is not properly guided. Also, if certain rotational limits in pitch, yaw, and roll are exceeded the stable platform will be forced out of its frame of reference thus causing the guidance measurements to be erroneous. These rotational limits will not apply to the four-gimbal ST-124 platform.

The engine deflection angles are the outputs of the control computer used to initiate the change in the thrust vector required to correct for flight-path deviations.

The power supply is monitored to provide a check for malfunctions due to loss of voltage. Also the frequency of the inverter, used to convert DC current to AC, is monitored to aid in determining failures in the electrical network.

2.1.4 Other Measurements

The performance of the inertial guidance system is subject to errors due to nonstandard environmental conditions and errors or failures in the electrical circuitry. To aid in determining the cause of any malfunction, vibration and temperature measurements are made in critical areas. Also measurements are made of the instrument-compartment pressure and the pressure supply to the air bearings. These pressures must remain within certain limits to insure proper guidance system performance. When evaluating the guidance system on a normal flight, these measurements need only be checked to insure that they remain within operational specifications.

2.2 External Tracking Data

The vehicle is tracked by various electronic and optical tracking systems which are independent of the guidance system. The data thus received are essentially earth-fixed positions with respect to time. The coordinate system is identical to that of the platform coordinates at the instant of launch with the origin remaining earth-fixed at the launch site.

These earth-fixed coordinates may be transformed into guidance indications as shown in Appendix B. The earth-fixed positions are transformed into inertial platform values and then a simple rotation is made through the standard elevation angle (ϵ) into the guidance coordinate system. By including any standard preset and/or programmed values in the transformation, guidance indications are computed which correspond to the outputs of the guidance computers.

The guidance values calculated from external tracking may be compared with the telemetered guidance indications and the differences used in determining errors made by the guidance system. These differences reflect random errors in tracking data and uncertainties incurred in establishing the trajectory as well as the guidance errors. It is therefore impractical to attempt to isolate errors that are within the accuracy of either data source compared.

The transformation and comparison process mentioned above has been programmed and utilized in the Computation Division of MSFC. An alternate approach to the data comparison would be a transformation of the inertially measured guidance quantities into earth-fixed values and then a comparison of these data with the corresponding earth-fixed measurements. This method would serve a two-fold purpose: first, the guidance errors in terms of earth-fixed components could be easily established and, second, continuous data would be available to establish a post-flight trajectory through areas not adequately covered by ground tracking facilities. However, the residuals obtained in the earth-fixed plumbline system may not be sufficient to determine accurately the source of guidance errors.

The derivation of the equations used to transform inertial measurements into earth-fixed plumbline components is presented in Appendix B. The gravitational components required in the transformations may be derived in two ways. Since the acceleration due to gravity is a function of the vehicle position with respect to the center of the earth, the gravitational components may be derived from earth-fixed positions. Also, the gravitational components may be determined from the measured inertial displacements through an iterative procedure if the vehicle position relative to the center of the earth is accurately known at some time point during this interval (e.g., the launch site at liftoff, ballistic camera tracking point, etc.).

3.0 GUIDANCE ERRORS

The outputs of the guidance computers will, of course, include any errors made in presetting the computers as well as those made during vehicle flight. The guidance errors during flight result from any non-standard alignment and/or performance of the guidance hardware. The total guidance errors may be determined by comparing the telemetered guidance indications with corresponding values derived from a tracking system independent of the guidance instrumentation. This comparison method is discussed in Paragraph 4.0.

An evaluation of the guidance system serves a two-fold purpose. First, the guidance deviations are used as input data for a least squares solution for guidance error sources and second, the deviations may be transformed into other coordinate systems to show the effect of guidance errors on injection parameters for an orbital flight or other conditions required to accomplish the desired mission.

3.1 General Classes of Guidance Error Sources

The telemetered guidance outputs include errors from known sources:

1. Stabilized platform errors
2. Accelerometer errors
3. Other hardware and circuitry errors

These are guidance system errors and contribute to deviations in the vehicle flight path. The schematic in Figure 4 shows how the hardware error sources contribute to the total errors in the measured guidance values. Drift of the stabilizing gyros and initial misalignments constitute the total platform alignment errors. These deviations together with the accelerometer errors result in biased accelerations. Outputs of the guidance accelerometers are sent through the guidance computer and finally result in the total errors in the guidance measurements. The biased measurements are utilized in the computations of guidance commands (steering, cutoff, etc.) which are sent to the control computer and system network.

In addition to the guidance system errors, the telemetered guidance data contain small random errors caused by telemetry and the necessary data reduction process. These errors do not affect the flight of the space vehicle but they should be considered in any solution for error sources.

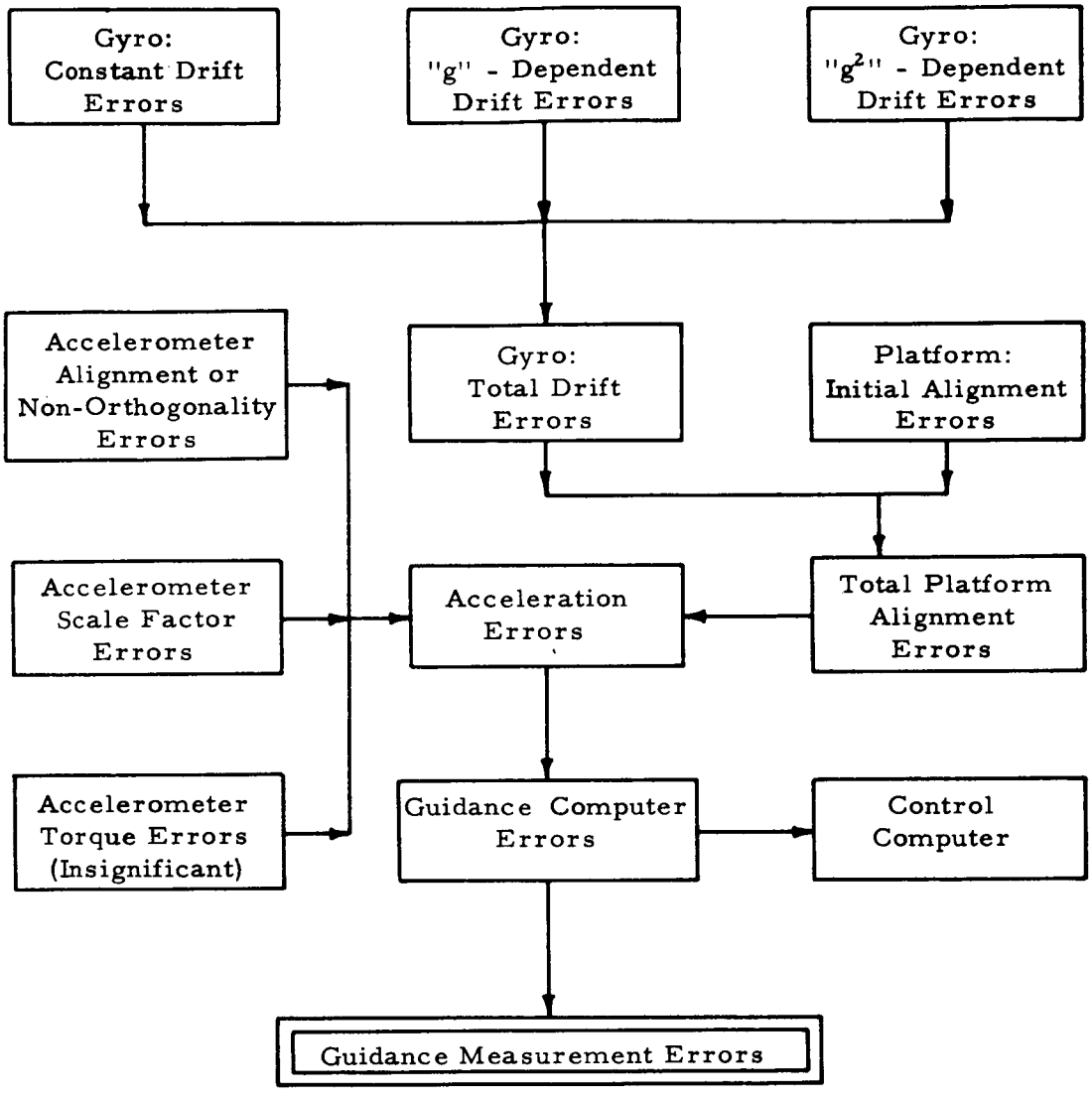

MTP-AERO-62-76

FIG. 4. CONTRIBUTION OF HARDWARE ERRORS TO TOTAL ERROR IN GUIDANCE MEASUREMENTS

3.2 Functional Errors

Functional guidance errors are defined as those caused by guidance system components not mounted on the stable element such as the guidance computer, signal processor, electrical circuitry, and other equipment. The specific hardware components and accuracy may vary somewhat depending on the mission to be accomplished.

Some typical functional errors are:

1. Presetting errors
2. Integration errors
3. Cutoff errors
4. Gearing errors (backlash, synchro, etc.)
5. Control errors from finite control gains

These errors are not all necessarily applicable or of the same magnitude for a particular guidance system. Presetting errors, for example, would not apply to a digital computer such as will be flown in the Saturn vehicles. However, if an analog computer is used, certain initial input data may be introduced by a preset voltage level to represent the desired value.

Integration errors are also greatly dependent on the type of computer flown. The digital computer again would eliminate errors caused by a lag in the mechanism. The integration error for a digital computer would essentially be limited to a time delay between actual liftoff and the time liftoff signal is executed.

Guidance cutoff errors generally result from a delay in time between computation and execution of a cutoff command. This error may be determined by inserting the proper guidance measurements made at cutoff signal into the cutoff equation. Any solution of the equation other than zero would constitute the error.

The control gain coefficients are predetermined values that may or may not vary with time of flight and are programmed in the vehicle prior to launch. Although errors in the control gains would be small, they do contribute to the total guidance error.

3.3 Guidance Intelligence Errors

The total guidance errors are defined as the differences between the positions and velocities measured by the guidance system and the corresponding flight coordinates with respect to ideal performance of

the guidance system. Ideal performance of the guidance system means, for this report, that the guidance hardware is properly aligned, remains fixed during flight, and no errors are made in sensing the vehicle accelerations or in integrating these accelerations into velocities and displacements. Since the computer errors may be determined from the telemetered data (par. 3.2), they may be removed from the guidance values. The remaining deviations are the results of platform and accelerometer errors. These deviations are referred to in this report as "guidance intelligence errors" and are used as input data for a least squares solution for the error sources.

Guidance intelligence errors cannot be detected from the telemetered measurements unless some major malfunction occurs. The sources of intelligence errors that produce very similar end results can be divided into four groups.

1. Misalignments

   a. Azimuth and leveling about the platform axes
   b. Nonorthogonality of each accelerometer with respect to the other two.

2. Constant Drifts

   a. Around all three platform axes

3. "g" - Dependent Drifts

   a. Around all three platform axes
   b. Scale factor error of all three accelerometers (negligible in cross range)

4. "g^2" - Dependent Drifts

   a. Around all three platform axes

An evaluation in terms of the guidance intelligence presents the problem of first determining the errors made and then solve for the error sources. This report is primarily concerned with a method of solving for the guidance intelligence error sources and the resultant deviations in injection conditions for an orbital flight.

4.0 GUIDANCE INTELLIGENCE ERROR ANALYSIS

The guidance intelligence errors are defined as deviations in the guidance measurements resulting from hardware errors. Intelligence errors are obtained by comparing the telemetered guidance system values with those calculated from trajectory data. By first screening the functional errors from the telemetered guidance outputs, the remaining differences obtained represent the guidance intelligence errors. Figure 5 presents the flow diagram of a least squares method of determining the sources of guidance intelligence errors.

The earth-fixed positions and velocities from the trajectory established from external tracking data are transformed into the respective guidance indications by using the standard alignment of the platform and accelerometers along with the appropriate computer presettings and programmed values. These calculated guidance values are compared with the telemetered outputs (functional errors eliminated) and the differences are residuals to be used as input data for a least squares solution for the individual error sources.

The basic equations relating the guidance intelligence errors to the hardware errors are:

$$(1). \quad R = \partial u$$

$$(2). \quad u = (\partial^T w \partial)^{-1} \partial^T w \, R$$

where R = (m by 1) residual matrix of guidance differences

∂ = (m by n) matrix of partial derivatives of guidance errors with respect to individual error sources

u = (n by 1) matrix of guidance error sources

w = (m by m) diagonal matrix consisting of weights assigned to the residuals

-1 superscript refers to matrix inverse

T superscript refers to matrix transpose

The matrix elements relating the velocity and displacement deviations to each of the error sources can be determined by using perturbation techniques with the usual equations of motion and the required coordinate transformation. The standard alignment angles for the platform and accelerometers as well as the one sigma values for the platform and accelerometer hardware errors are used as inputs in

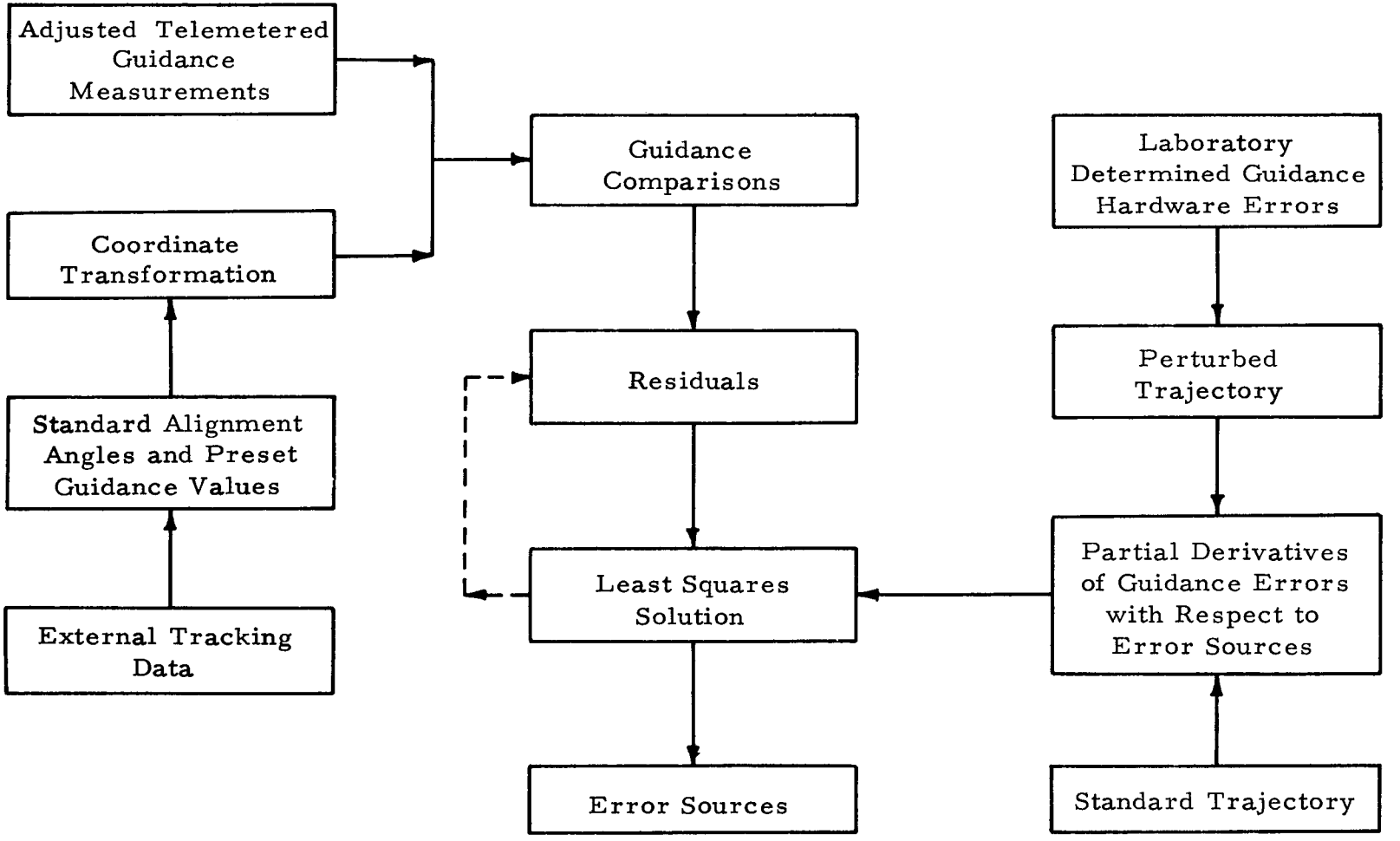

FIG. 5. GUIDANCE INTELLIGENCE ERROR ANALYSIS

computing the partial derivative matrix elements. The equations for this procedure are presented in Appendix C. After the partial derivative matrix elements and the guidance errors have been determined, an initial least squares solution is obtained for the error sources. The first results (u) are then inserted in equation (1) and R' is calculated.

Then $\Delta R = R - R'$

Equation (2) then becomes

$$\Delta u = (\partial^T_w \partial)^{-1} \partial^T_w \Delta R$$

$$u = u' + \Delta u$$

This iterative procedure is continued until R' converges to R within the limits specified by the weights assigned to the guidance measurements.

4.1 Comparison of Guidance Errors

The many combinations of errors in data available for evaluating the guidance ystem make it extremely difficult to determine the sources of relatively small guidance errors. To illustrate this, trajectories were first calculated individually introducing known error sources. Then, guidance indications from these calculations were compared with corresponding ideal values for the two-stage flight. Error profiles for the first stage and for total flight are presented in Figures 6 through 15 in the following order:

Error Source		Effective Velocity Errors	Figure No. 1st Stage	Figure No. Total Flight
Platform Errors -				
Rotations about:	X-axis	cross range	6	7
	Y-axis	cross range	8	9
	Z-axis	slant altitude	10	11
		slant range	12	13
Accelerometer Errors -				
Cross Range		cross range	14	15
Slant Altitude		slant altitude		
Slant Range		slant range		

The guidance velocity errors for both first stage and total flight are plotted as percent of total error at "end of first stage thrust" versus percent of burning time. These figures clearly show the error buildup resulting from each source. It is not to be assumed that the ultimate velocity errors are necessarily of the same magnitude in each case. Their magnitudes, in fact, are quite different. By using percentages the different curves are easily established even for small errors where absolute values could not be plotted on a usable scale. The entire profile must be considered in any attempt to separate the error sources.

Cross-range velocity errors produced by the four types of errors around the platform X-axis are shown in Figure 6 for the first stage. The error resulting from an initial misalignment is clearly distinguished from any other. No other error source could be distinguished until after fifty percent of the burning time. The separation between the error sources is more distinct between 60% and 90% of the burning time. The maximum difference between any two curves other than initial misalignment is 38% of the total error at about 75% of the burning time.

Figure 7 shows these cross range velocity errors for the total flight. The velocity errors continue to increase until about 70% of the total burning time. From this point the cross range accelerometer picks up negative Y-acceleration thus reducing the positive error built up in cross range velocity. The cross range velocity error at the end of the second stage would be approximately the same as the error at first stage cutoff for an initial platform misalignment and drifts influenced by accelerations in the Y direction. Other drifts about the X-axis would practically cancel out their cross range velocity error by the end of second stage.

The cross range velocity errors in the first stage resulting from rotations about the platform Y-axis are shown in Figure 8. Again the initial misalignment error is the more distinct though the buildup is negligible before 50% of first stage burning time. The error sources about the Y-axis are more difficult to distinguish for small differences than those about the X-axis. The maximum difference between any two curves except the initial misalignment is 25% at about 80% of burning time. These errors are shown for the total flight in Figure 9. Since a platform misalignment about the Y-axis is essentially an azimuth error, the cross range velocity errors continue to increase during the second flight stage. Toward the end of flight it would be easier to distinguish between error sources.

Figure 10 shows the slant altitude velocity errors in the first stage resulting from rotations about the platform Z-axis. The initial misalignment error profile is more distinct than the other curves which show little or no significant error until after 50% of first stage burning time. The maximum difference between any two curves except initial misalignment is 32% of the total error at about 80% of burning time. Similar errors in slant altitude velocity are shown for the total burning time in Figure 11. The errors continue to increase during the second stage with the error sources becoming more distinct toward the end of flight. Still, the error profiles of "g" - dependent and "g^2"-dependent drifts are essentially the same.

The percentage errors in slant range velocity for the first stage, caused by platform errors about the Z-axis, are shown in Figure 12. The errors generated by an initial misalignment may be easily distinguished from other platform errors, but it would be extremely difficult to isolate any other platform error source. The velocity errors generated by drift proportional to acceleration in the X direction were found to be insignificant in the first stage of flight. However, Figure 13 shows the slant range velocity errors for the total flight and indicates that these errors may become quite significant by the end of second stage.

All the velocity errors build up during the first stage and change direction during the second stage which would tend to cancel out first stage errors. Due to a longer burning time in the second stage, the velocity errors caused by platform drift may become very significant by the end of second stage thrust. Individual error sources are more easily isolated toward the end of second stage burning.

First stage guidance velocity errors resulting from accelerometer error sources are presented in Figure 14 as percent of total error at end of first stage thrust versus percent of burning time. The profiles are identical for guidance velocity errors generated by the cross range and slant range accelerometers nonorthogonal with respect to the slant altitude accelerometer and slant altitude scale factor error. Also identical error profiles result from the cross range and slant altitude accelerometers nonorthogonal with respect to the slant range accelerometer and the slant range scale factor error. From Figure 15 it may be noted that velocity deviations in the second stage caused by accelerometer errors are grouped essentially the same as in the first stage. One group (slant range scale factor, slant altitude and cross range accelerometer misalignments about the ζ and η axes respectively) increases with time. The second error group (slant altitude scale factor, slant range and cross range accelerometer misalignments about ζ and ξ axes respectively) decrease in the second stage and may build up errors of opposite sign to the corresponding velocity errors at end of first stage thrust. Since the acceleration in the cross range direction would be very small, the scale factor error for this accelerometer is negligible.

The error profiles presented in Figures 6 through 15 are general and will vary somewhat with different trajectories to be flown and changes in accelerometer orientations. However, a similar system of error profiles may be easily established for any given trajectory and/or accelerometer orientation. Also, a comparison of the various error profiles will give an idea of the difficulty in isolating small error sources. Some errors tend to cancel others which should be expected for an actual flight. It was assumed that all errors were additive in trajectory computations for this report.

The summation of the one sigma (1σ) guidance intelligence errors at second stage cutoff in terms of earth-fixed positions and velocities is:

$$\Delta X_e = \mp 1009 \text{ m} \quad ; \quad \Delta \dot{X}_e = \mp 1.5 \text{ m/s}$$

$$\Delta Y_e = \pm 679 \text{ m} \quad ; \quad \Delta \dot{Y}_e = 3.1 \text{ m/s}$$

$$\Delta Z_e = \pm 1405 \text{ m} \quad ; \quad \Delta \dot{Z}_e = 3.6 \text{ m/s}$$

and in terms of injection parameters:

$$\Delta R = \pm 422 \text{ m} \quad ; \quad \Delta \alpha_v = \pm 0.023 \text{ deg}$$

$$\Delta V_e = \mp 2.1 \text{ m/s} \quad ; \quad \Delta \psi = \mp 0.010 \text{ deg}$$

$$\Delta \epsilon_v = \pm 0.012 \text{ deg} \quad ; \quad \Delta \lambda = \mp 0.012 \text{ deg}$$

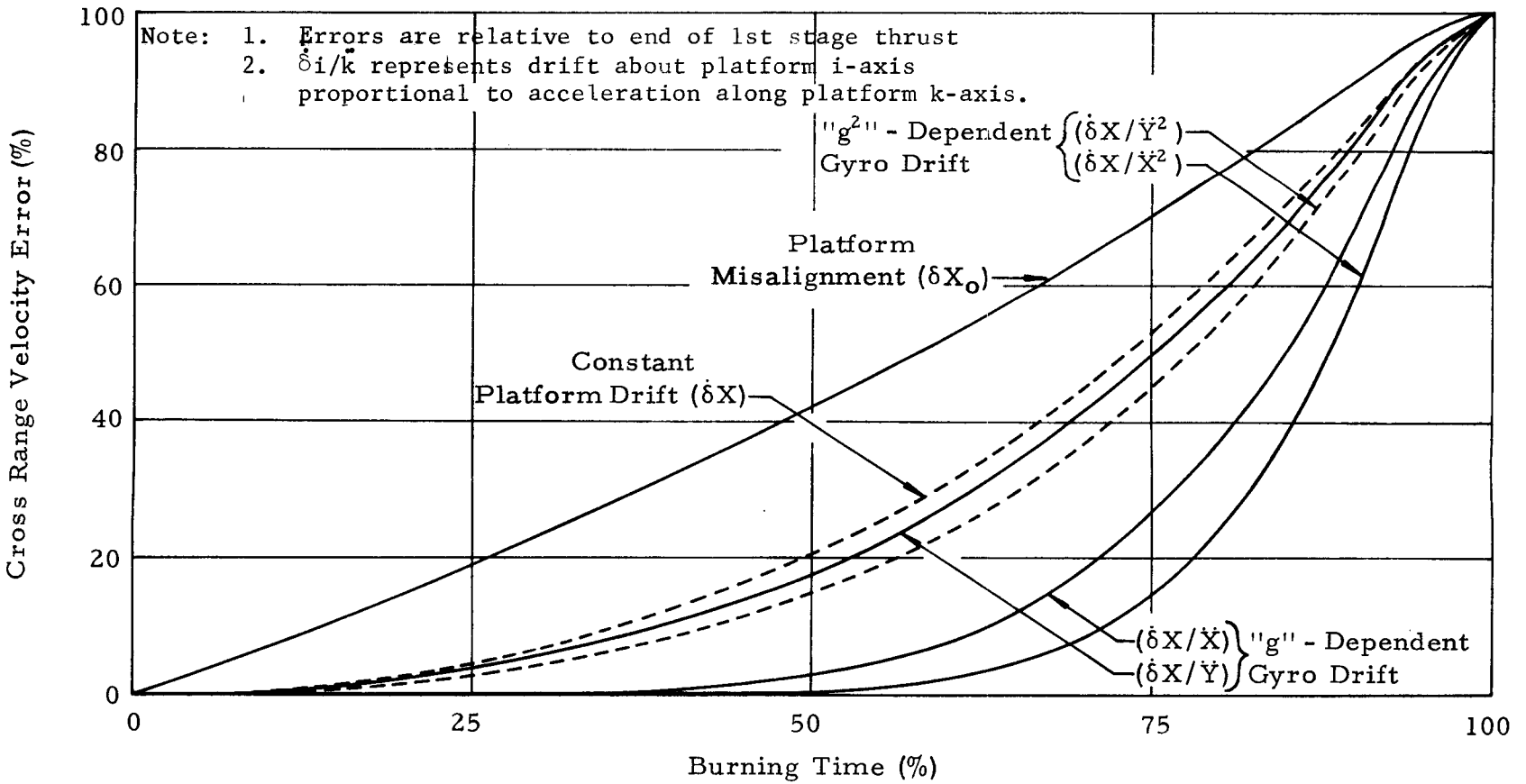

MTP-AERO-62-76

FIG. 6. CROSS RANGE VELOCITY ERRORS (FIRST STAGE)
RESULTS OF ALIGNMENT ERRORS ABOUT X-AXIS

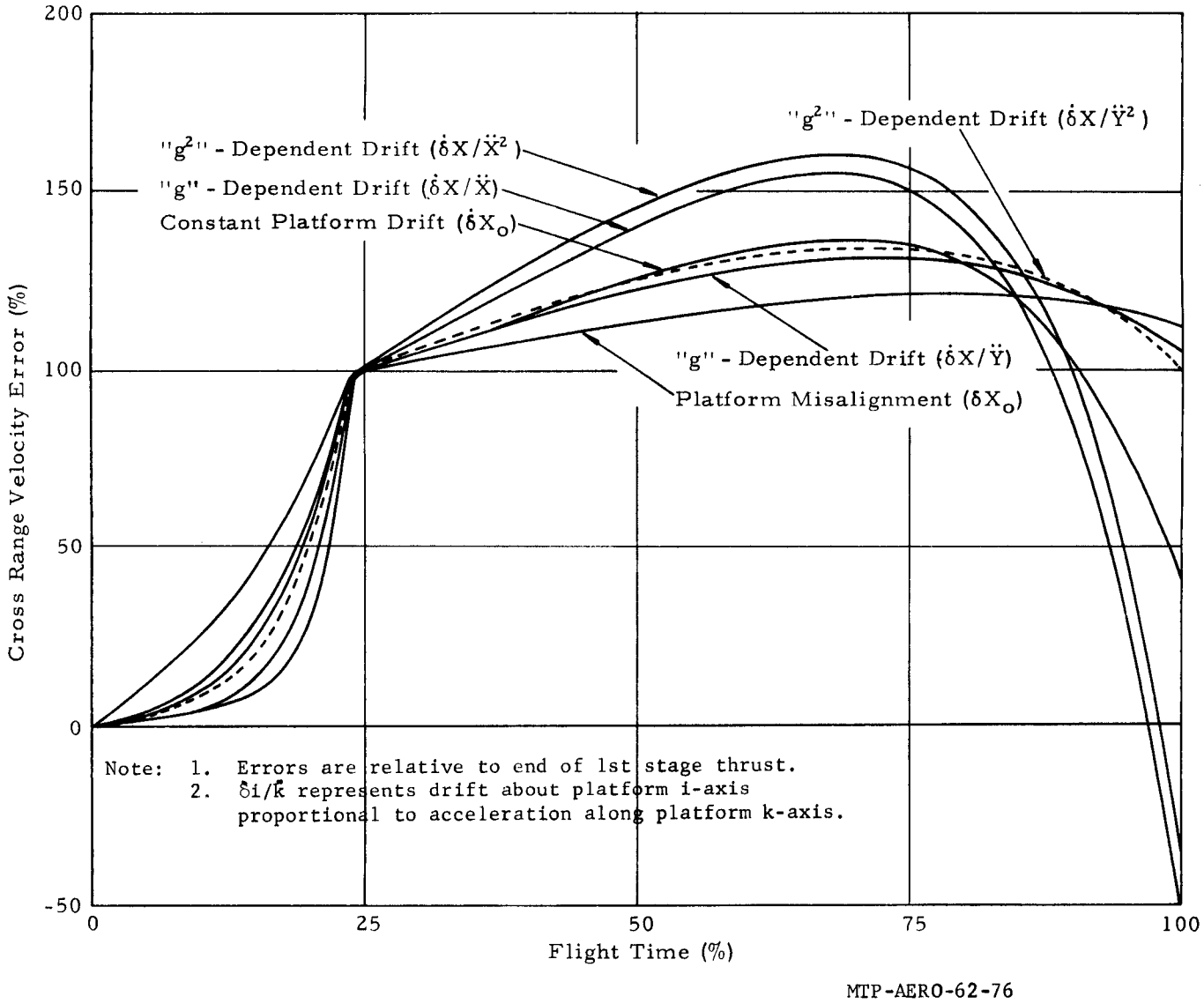

FIG. 7. CROSS RANGE VELOCITY ERROR (TOTAL FLIGHT)
RESULTS OF ALIGNMENT ERRORS ABOUT X-AXIS

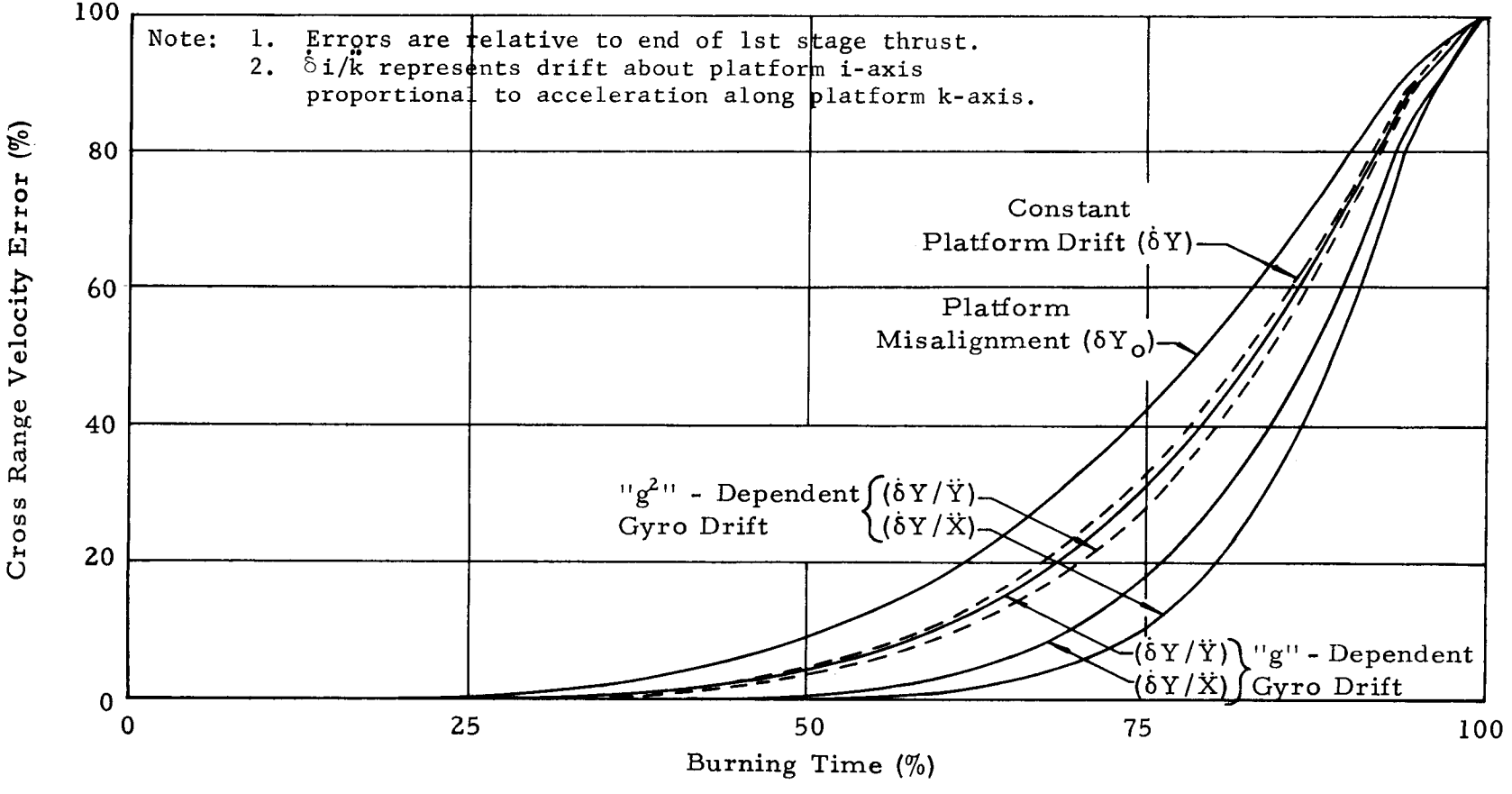

MTP-AERO-62-76

FIG. 8. CROSS RANGE VELOCITY ERRORS (FIRST STAGE)
RESULTS OF ALIGNMENT ERRORS ABOUT Y-AXIS

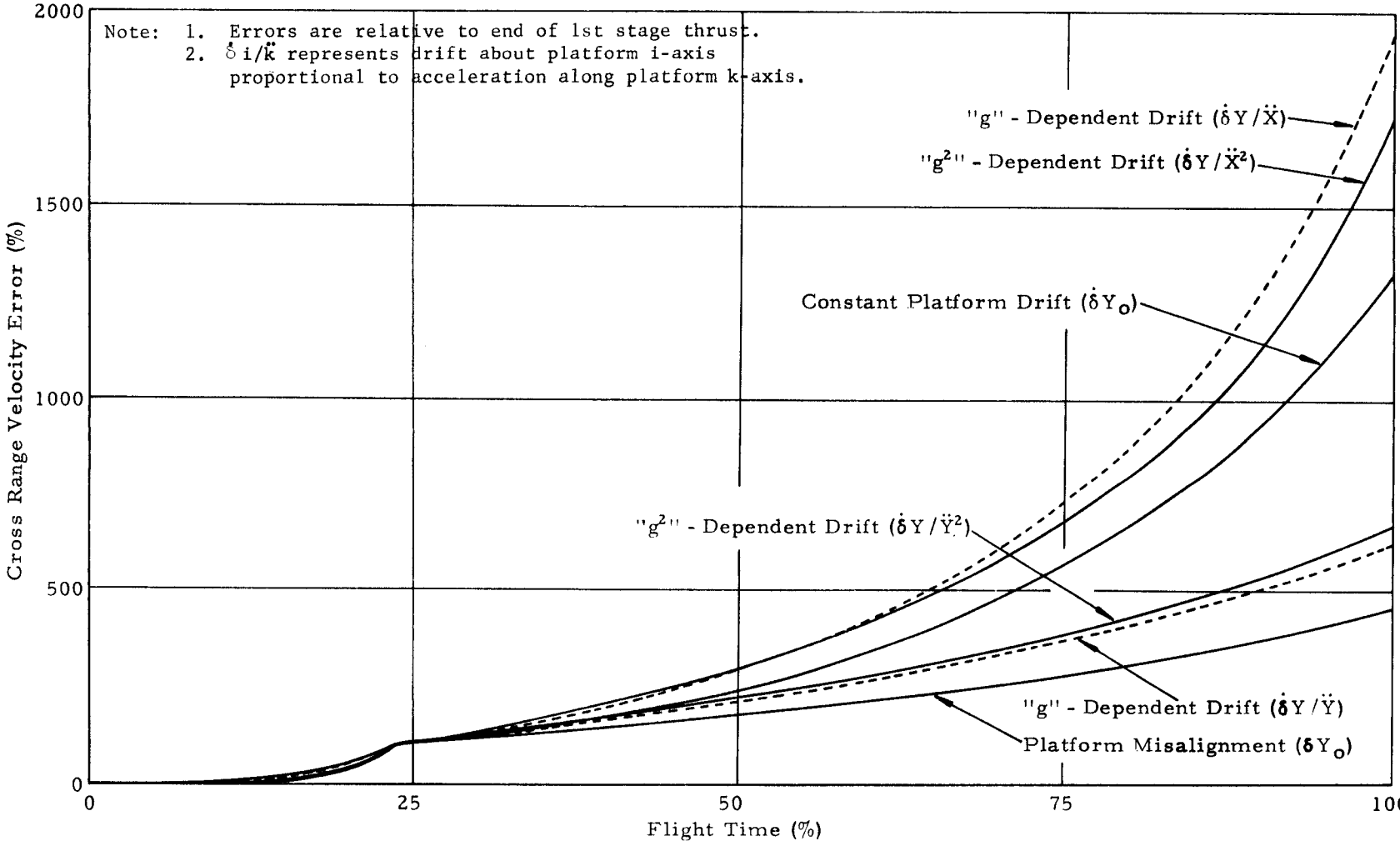

FIG. 9. CROSS RANGE VELOCITY ERRORS (TOTAL FLIGHT)
RESULTS OF ALIGNMENT ERRORS ABOUT Y-AXIS

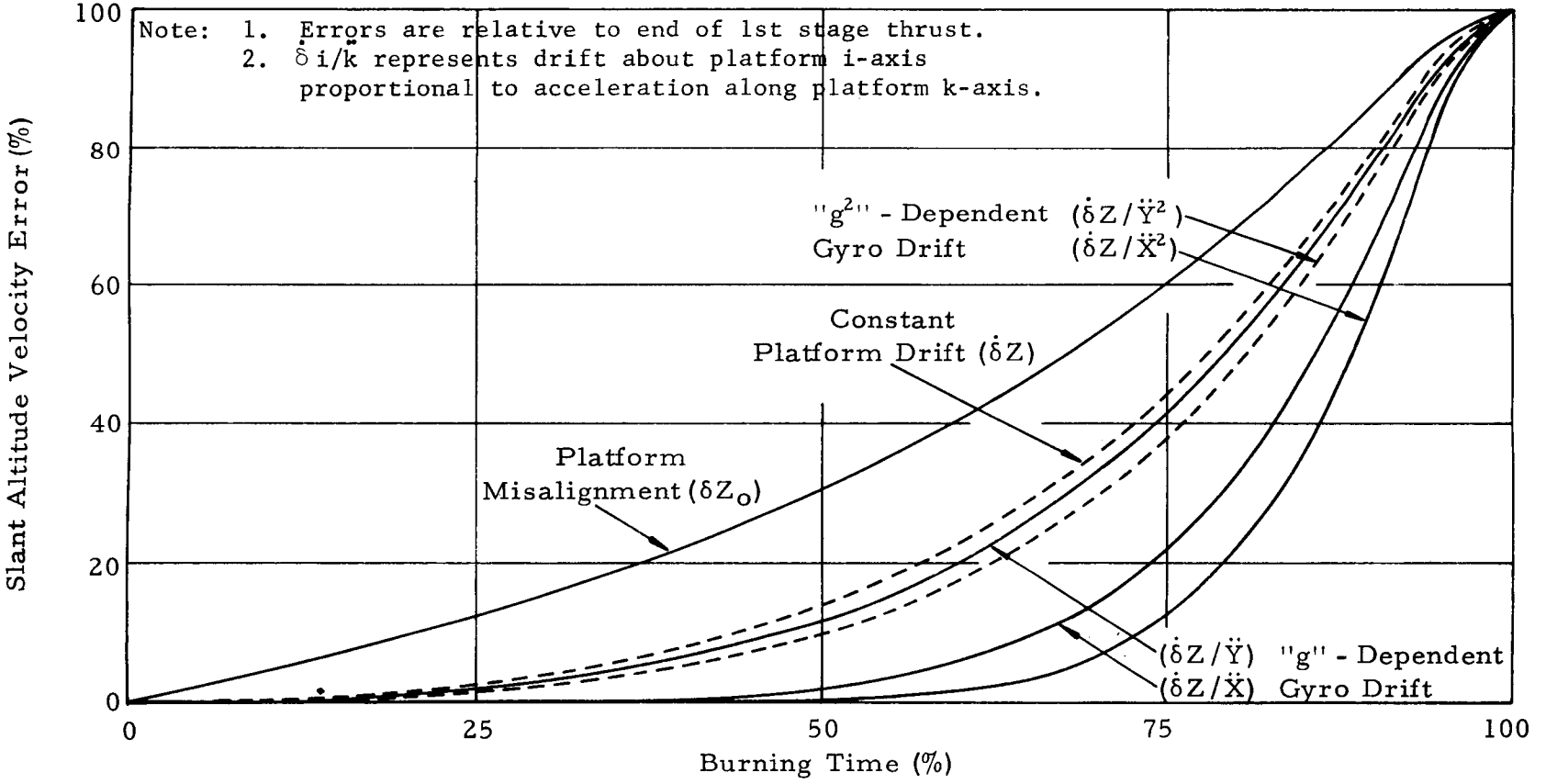

MTP-AERO-62-76

FIG. 10. SLANT ALTITUDE VELOCITY ERRORS (FIRST STAGE) RESULTS OF ALIGNMENT ERRORS ABOUT Z-AXIS

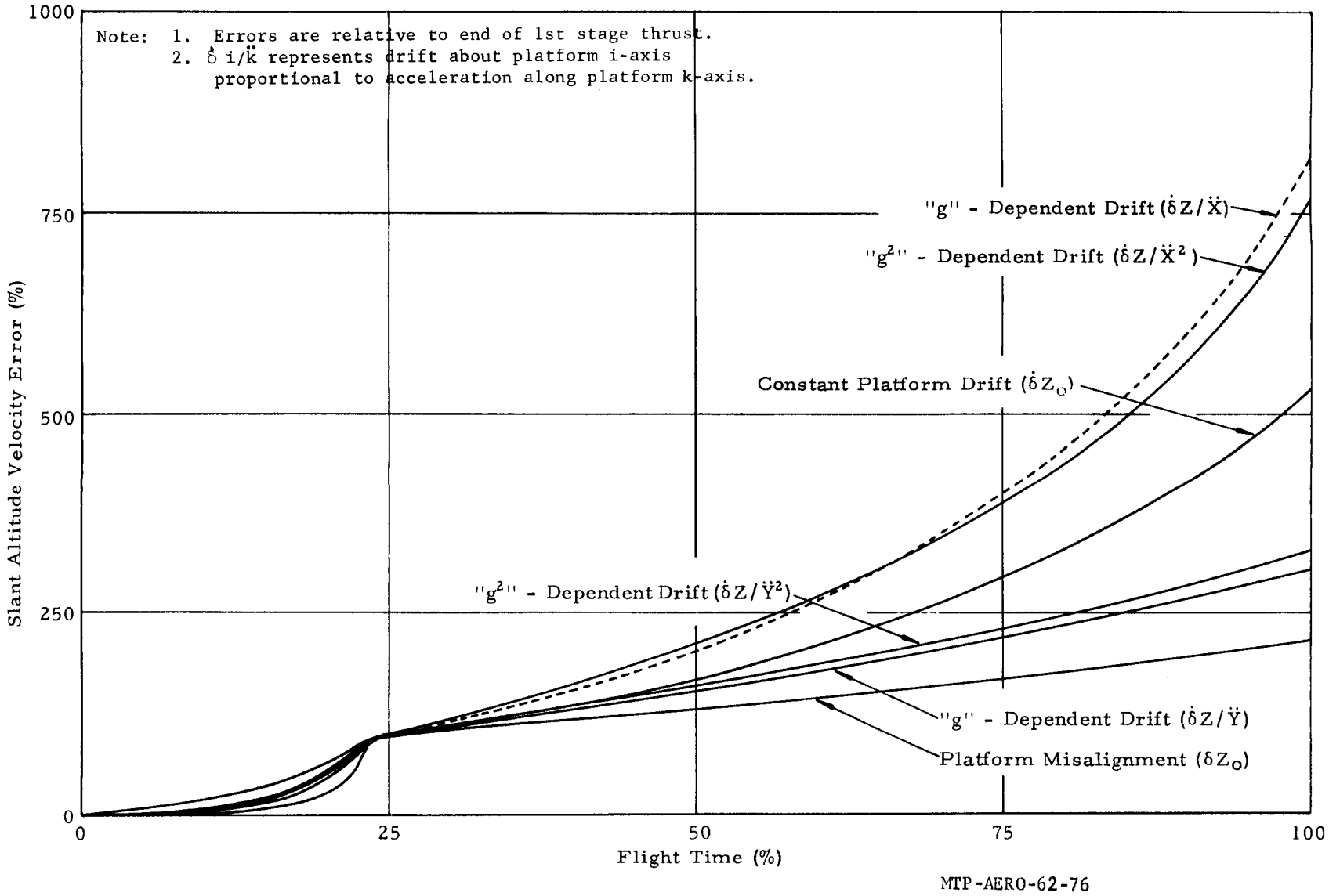

MTP-AERO-62-76

FIG. 11. SLANT ALTITUDE VELOCITY ERRORS (TOTAL FLIGHT) RESULTS OF ALIGNMENT ERRORS ABOUT Z-AXIS

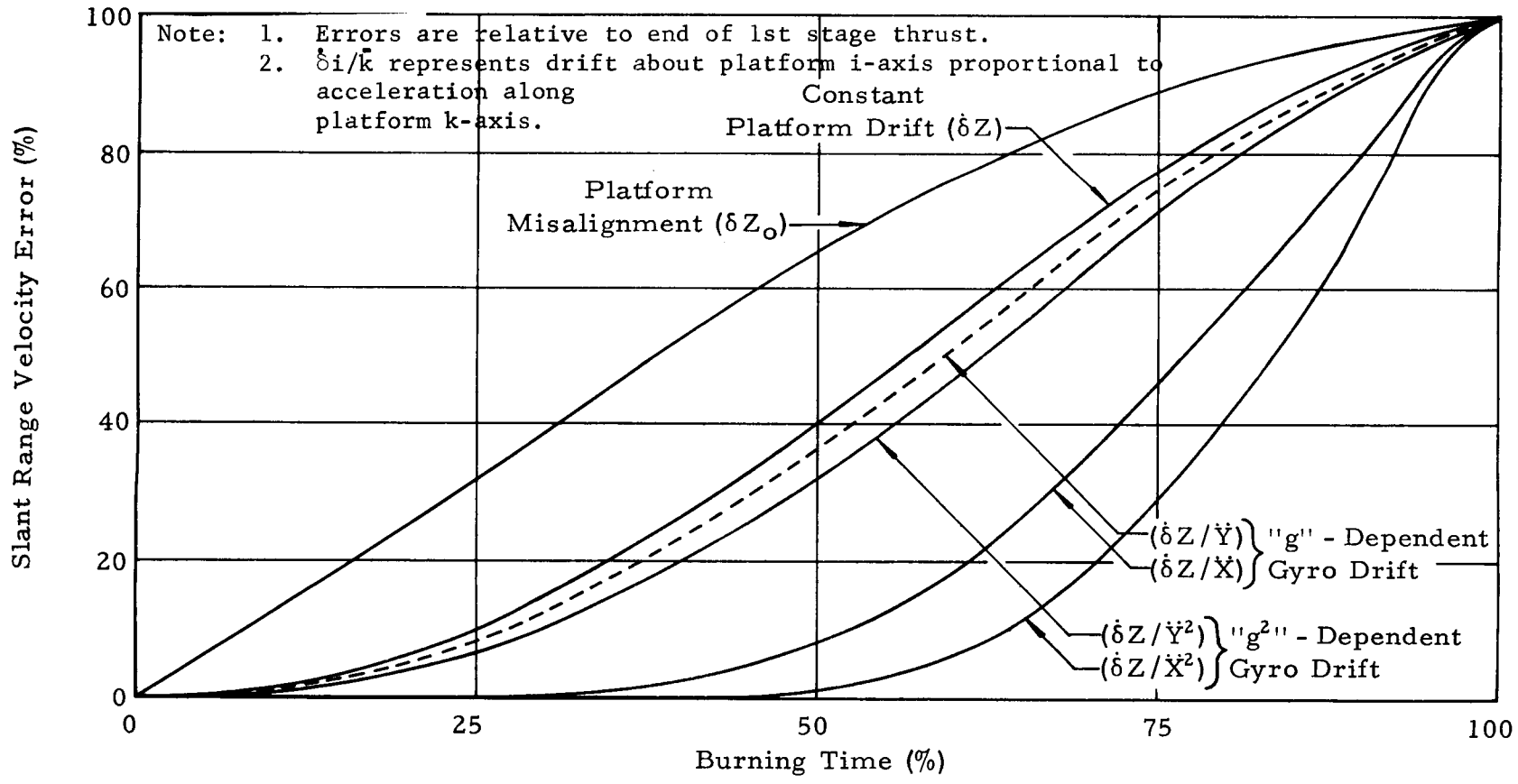

MTP-AERO-62-76

FIG. 12. SLANT RANGE VELOCITY ERRORS (FIRST STAGE) RESULTS OF ALIGNMENT ERRORS ABOUT Z-AXIS

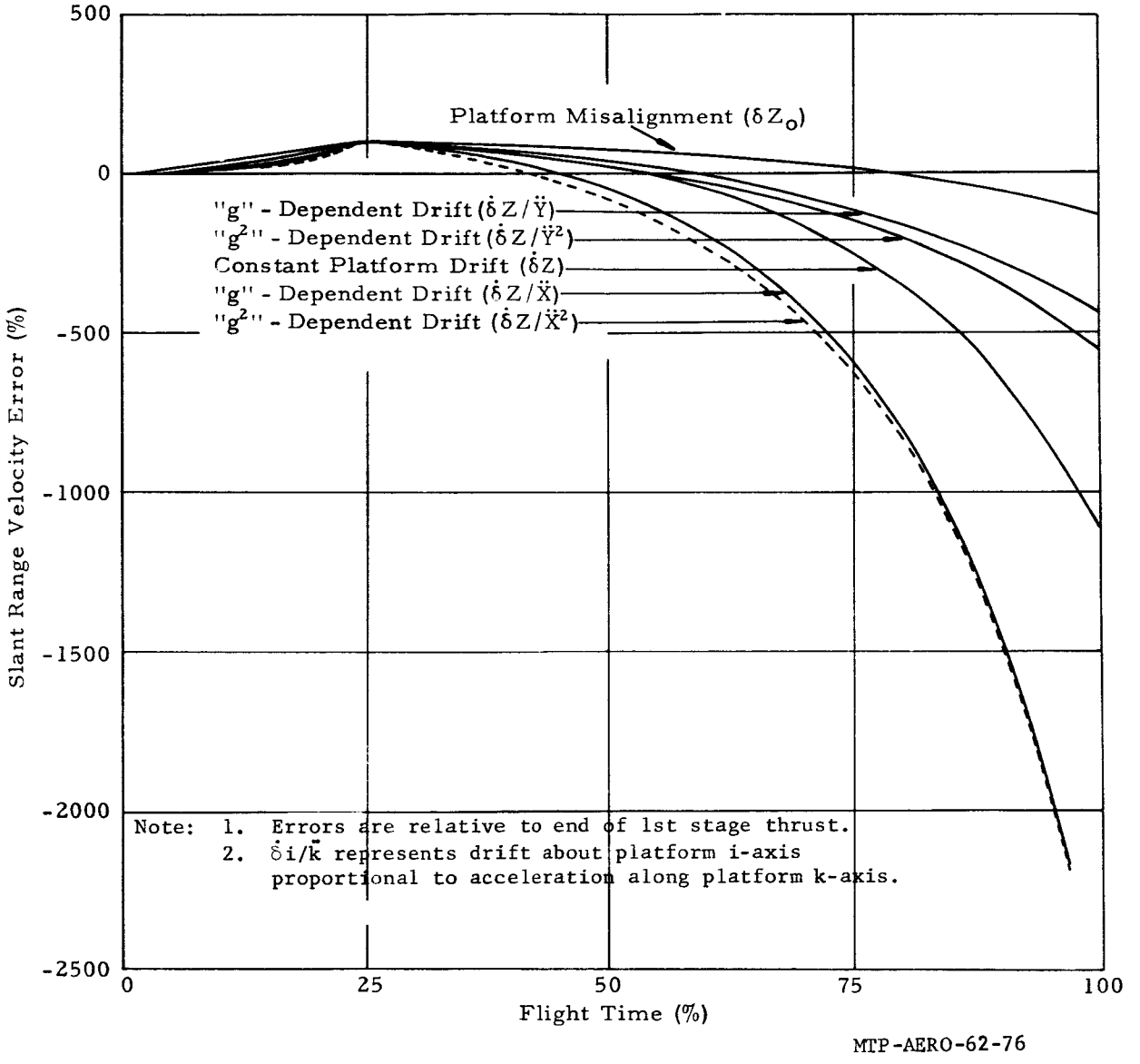

FIG. 13. SLANT RANGE VELOCITY ERRORS (TOTAL FLIGHT)
RESULTS OF ALIGNMENT ERRORS ABOUT Z-AXIS

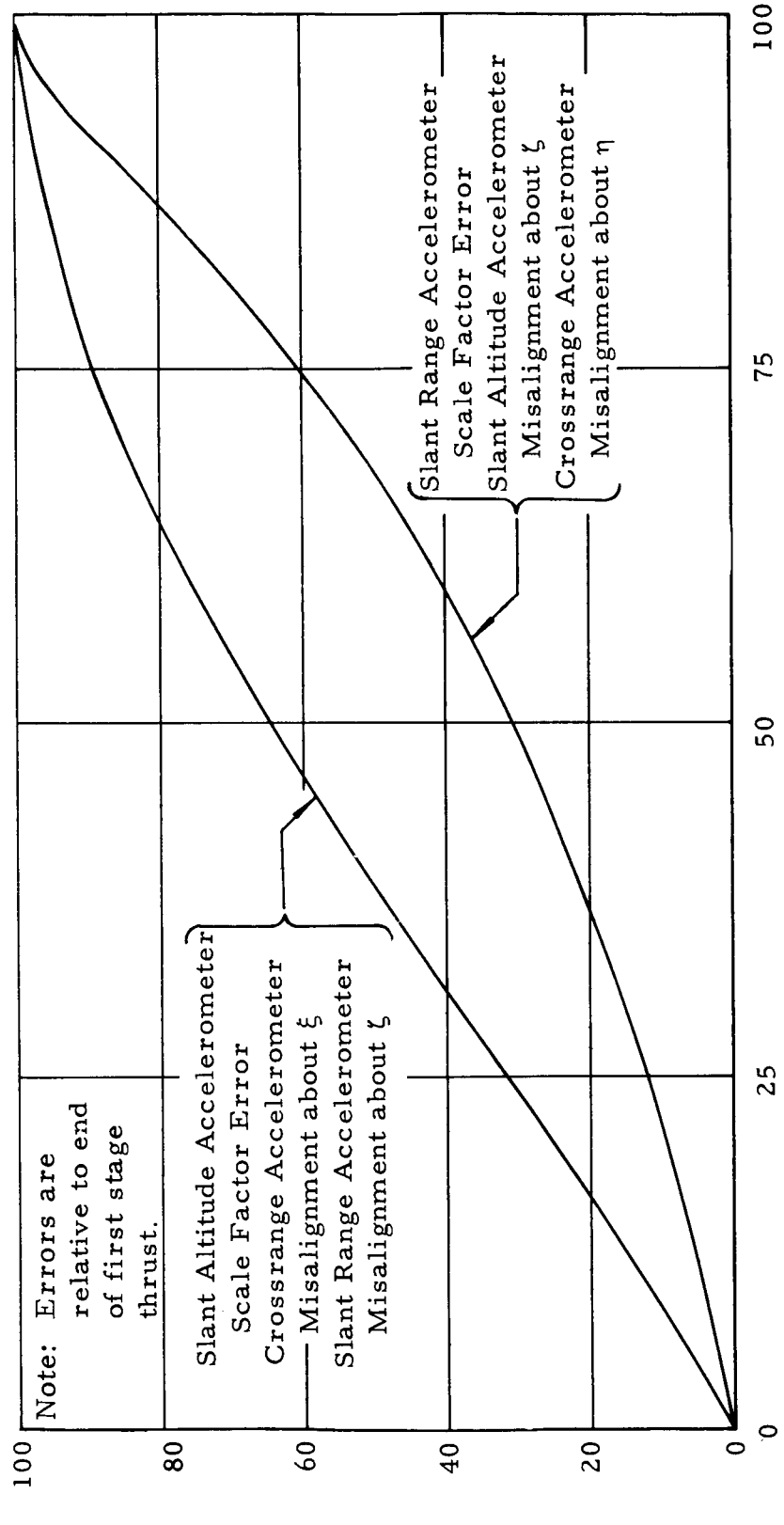

MTP-AERO-62-76

FIG. 14. GUIDANCE VELOCITY ERRORS (FIRST STAGE)
RESULTS OF ACCELEROMETER ERRORS

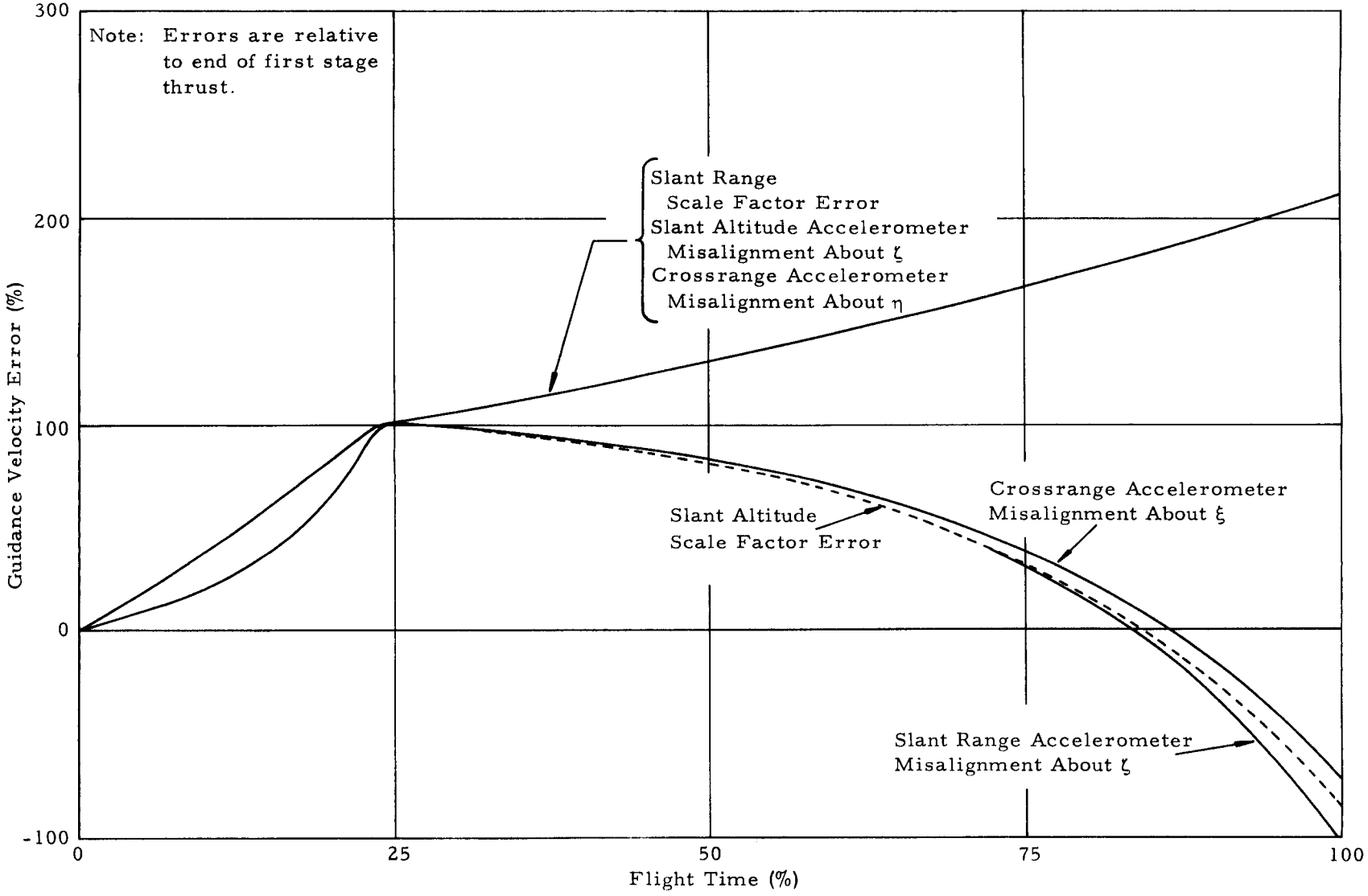

MTP-AERO-62-76

FIG. 15. GUIDANCE VELOCITY ERRORS (TOTAL FLIGHT) RESULTS OF ACCELEROMETER ERRORS

APPENDIX A

1. Guidance Error Contributions to Errors in Earth-Fixed Plumbline Coordinates

The guidance system is designed to obtain information during flight as to the local state (time, thrust acceleration, position, and velocity), make a decision based on this information as to how the vehicle should be steered, carry out the required maneuvers, and finally terminate thrust at the proper instant. However, errors resulting from the guidance system are not corrected. The results of the individual guidance errors were simulated by perturbation techniques. The guidance system errors introduced into the trajectory calculations were the 1 sigma (1σ) values for all hardware error sources plus increasing each error source individually such that the guidance velocity errors at first stage cutoff would be normalized at:

$\Delta\dot{\zeta}$ = 10 m/s

$\Delta\dot{\eta}$ = 10 m/s

$\Delta\dot{\xi}$ = -1.5 m/s

Effects of the guidance system errors on the outputs of the accelerometers were assumed to be additive. The velocity errors were normalized at values large enough to easily distinguish between the results yet remain linear with respect to the individual error source. It is not to be construed that errors of such magnitude are to be expected of the guidance system. The slant range velocity error was chosen opposite in sign to the slant altitude thereby reducing the number of trajectory calculations.

Deviations about the platform X and Y axes result in cross range guidance errors but have negligible effect in either slant range or slant altitude directions. The cross range velocity error at first stage cutoff was normalized at 10 m/s for these calculations.

Guidance system errors about the platform Z axis affect both slant range and slant altitude with negligible effect in the cross range direction. These calculations were made such that the slant altitude velocity was 10 m/s at first stage cutoff. The effects in slant range velocity varied from the results of the total 1σ deviations to approximately -4.7 m/s for the platform misalignment about the Z axis.

The slant range velocity was normalized at -1.5 m/s for the accelerometer errors only (scale factor and nonorthogonality). The probability is negligible that the guidance system would experience a

TABLE III

EARTH-FIXED POSITION AND VELOCITY DIFFERENCES AT FIRST STAGE CUTOFF DUE TO NORMALIZED GUIDANCE INTELLIGENCE ERRORS

Multiple of 1σ Guidance Error Source	ΔX_e (meters)	ΔY_e (meters)	ΔZ_e (meters)	$\Delta \dot{Z}_e$ (m/s)	$\Delta \dot{Y}_e$ (m/s)	$\Delta \dot{Z}_e$ (m/s)
Total 1σ Values Only	-57	10	60	-1.1	0.3	1.3
Initial Platform Misalign.:						
(13.62) δ_X	-57	9	519	-1.1	0.3	10.0
(29.60) δ_Y	-59	10	311	-1.2	0.3	10.0
(14.55) δ_Z	-539	128	60	-10.1	4.5	1.3
Constant Gyro Drift:						
(143.79) $\dot{\delta}_X$	-57	10	378	-1.1	0.3	10.0
(248.01) $\dot{\delta}_Y$	-58	10	275	-1.1	0.3	10.0
(139.88) $\dot{\delta}_Z$	-346	134	60	-9.1	5.4	1.3
"g" - Dep. Gyro Drift:						
(654.55) $\dot{\delta}_X/\ddot{X}$	-57	10	247	-1.1	0.3	10.0
(176.81) $\dot{\delta}_X/\ddot{Y}$	-57	10	358	-1.1	0.3	10.0
(903.95) $\dot{\delta}_Y/\ddot{X}$	-57	10	212	-1.2	0.3	10.0
(287.57) $\dot{\delta}_Y/\ddot{Y}$	-58	10	266	-1.1	0.3	10.0
(578.96) $\dot{\delta}_Z/\ddot{X}$	-209	115	60	-8.2	6.1	1.3
(167.98) $\dot{\delta}_Z/\ddot{Y}$	-324	132	60	-8.9	5.5	1.3
"g^2" - Dep. Gyro Drift:						
(806.00) $\dot{\delta}_X/\ddot{X}2$	-57	10	207	-1.1	0.3	10.0
(156.90) $\dot{\delta}_X/\ddot{Y}2$	-57	10	339	-1.1	0.3	10.0
(1030.96) $\dot{\delta}_Y/\ddot{X}2$	-58	10	193	-1.2	0.3	10.0
(239.16) $\dot{\delta}_Y/\ddot{Y}2$	-58	10	257	-1.1	0.3	10.0
(687.81) $\dot{\delta}_Z/\ddot{X}2$	-173	101	60	-8.0	6.3	1.3
(145.08) $\dot{\delta}_Z/\ddot{Y}2$	-302	130	60	-8.8	5.6	1.3
Accelerometer Nonorthog.:						
(2.73) $\delta_{\eta\zeta}$	-103	-29	60	-1.8	-0.2	1.3
(14.55) $\delta_{\xi\zeta}$	-319	311	60	-7.0	7.1	1.3
(16.63) $\delta_{\xi\eta}$	-57	10	554	-1.1	0.3	10.0
Accelerometer Scale Factor:						
(2.42) C $\ddot{\xi}$	-87	-15	60	-1.8	-0.2	1.3
(51.30) C $\ddot{\eta}$	-464	478	60	-7.0	7.1	1.3

Note: (1) $\dot{\delta}_i/k$ represents drift about the i-axis proportional to acceleration in k direction.

(2) Errors of such magnitude as used in most of these computations are not to be expected of the guidance systems to be employed on the Saturn flights.

platform drift around the Z-axis sufficient to cause 1.5 m/s error in the slant range velocity if the accelerometers are aligned such that the slant range velocity vector would be approximately parallel to the vehicle trajectory at end of tilt. The calculations were based on the ST-90 guidance system and the standard alignments used in the Saturn Block I vehicle.

The earth-fixed position and velocity errors at end of the first stage thrust caused by the guidance deviations are shown in Table III. The differences were taken at standard outboard engine cutoff time thus eliminating gravitation effects due to a time differential. The guidance deviations used for Table III were intentionally increased to values much larger than any expected deviation in order to show the effect of the error in position and velocity components more clearly.

Figure 16 shows the differences in earth-fixed positions and velocities at first stage cutoff due to cross range guidance errors. The earth-fixed velocity error, $\triangle\dot{Z}_e$, was the same as the normalized error in cross range velocity, 10 m/s in each case except for the 1σ errors which produced 1.3 m/s error in $\dot{Z}_e$. The differences in X_e and Y_e were essentially the same for all cases or merely the results of the 1σ guidance errors. The errors in Z_e, at first stage cutoff, resulting from rotations about the X axis are somewhat larger than those caused by similar rotations about the Y axis.

The effect of a scale factor error for the cross range accelerometer is negligible and is not considered except in the total 1σ error calculations.

Figure 17 presents the earth-fixed position and velocity errors resulting from guidance system errors affecting slant range and slant altitude guidance. The nonorthogonal accelerometer, scale factor, and initial misalignment are the more significant errors to be expected from either slant range or slant altitude. In all cases affecting the slant altitude guidance measurements, the errors in both $\dot{X}_e$ and $\dot{Y}_e$ were significant and opposite in sign. However, the accelerometer errors affecting slant range only cause negligible deviations in $\dot{Y}_e$.

2. Effects of Guidance Deviations in Ephemeris Coordinate System

The ephemeris coordinate system is defined as an earth-fixed, right handed, Cartesian coordinate system with the origin at the center of the earth. Figure 18 illustrates the earth-fixed ephemeris coordinate system. The positive X-axis is directed through the 0° meridian at 0 hours Greenwich time; the positive Y-axis is directed through the 90° E meridian at 0 hours Greenwich time; and the positive Z axis is directed north along the earth's rotational axis. The

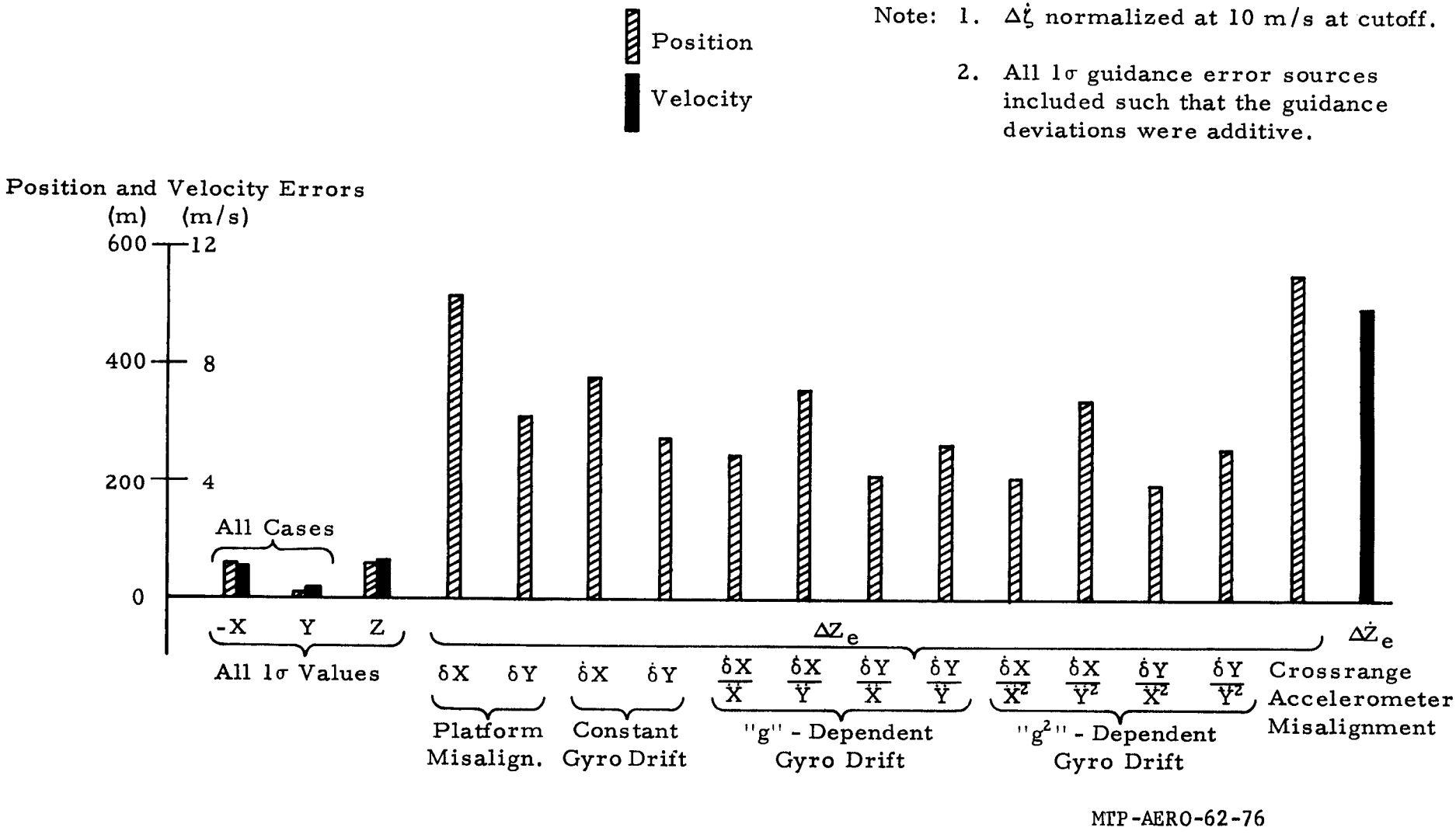

FIG. 16. EARTH-FIXED POSITION AND VELOCITY DEVIATIONS AT OUTBOARD ENGINE CUTOFF DUE TO GUIDANCE ERRORS ABOUT X AND Y AXES

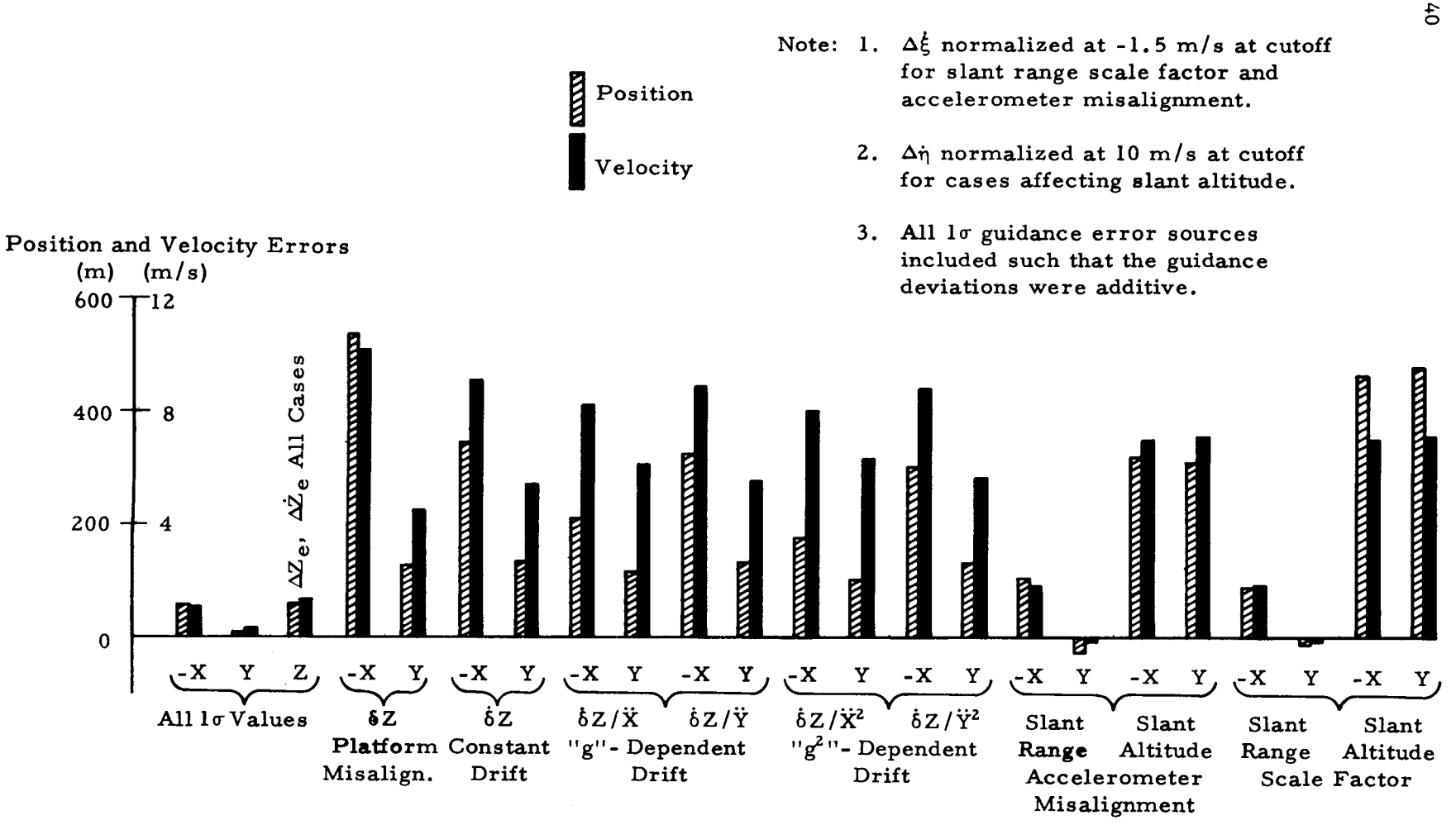

MTP-AERO-62-76

FIG. 17. EARTH-FIXED POSITION AND VELOCITY DEVIATIONS AT OUTBOARD ENGINE CUTOFF DUE TO GUIDANCE ERRORS ABOUT Z-AXIS

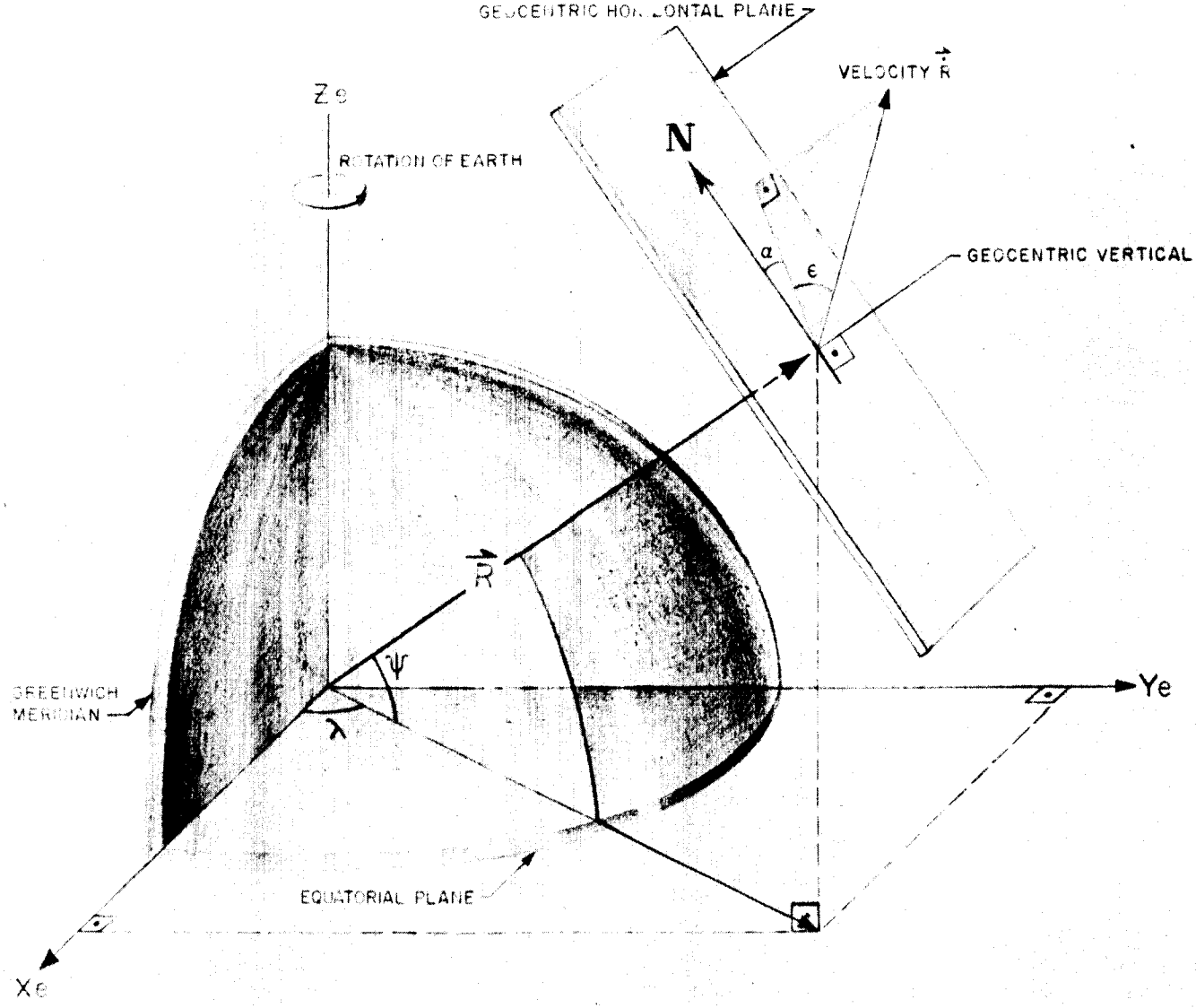

MTP-AERO-62-76

FIG. 18. EARTH-FIXED ÈPHEMERIS COORDINATE SYSTEM

matrix transformations from the earth-fixed (launch site origin) to ephemeris coordinate system and from inertial guidance coordinate system to ephemeris coordinate system are give in Appendix D.

The parameters of interest in the ephemeris coordinate system are:

1.	R	Radial distance from center of earth
2.	V_e	Earth-fixed velocity
3.	ϵ_v	Local elevation angle of velocity vector
4.	α_v	Local azimuth of velocity vector
5.	ψ	Geocentric latitude
6.	λ	Longitude

Perturbed trajectories were calculated for a 555 km orbital flight. The guidance system errors introduced into the trajectory calculations were the 1 sigma (1σ) values for all hardware error sources plus increasing each error source individually so that the guidance velocity errors at first stage engine cutoff would be normalized at:

$$\Delta\dot{\zeta} = 10 \text{ m/s}$$
$$\Delta\dot{\eta} = 10 \text{ m/s}$$
$$\Delta\dot{\xi} = -1.5 \text{ m/s}$$

Displacement errors were the results of the velocity deviations. Effects of the guidance system errors on the outputs of the accelerometers were assumed to be additive.

The inertial coordinates resulting from guidance intelligence errors were transformed into the injection parameters and compared with corresponding ideal values. These differences taken at second stage cutoff are presented in Table IV. The guidance system errors used for Table IV were intentionally increased to values much larger than any expected deviation in order to show the effect of the error in the parameters more clearly.

The significant injection parameter deviations as results of cross range guidance errors are azimuth, latitude, and longitude in that order. Errors in elevation, velocity, radial distance, and longitude are significant results of range and altitude guidance deviations.

The covariance matrix of the injection parameters that are a result of the various error sources in the guidance system was obtained from the usual equation

$$N = CUC^T$$

TABLE IV

INJECTION PARAMETER ERRORS DUE TO NORMALIZED GUIDANCE INTELLIGENCE ERRORS

Multiple of 1σ Guidance Error Source	Δ_R (meters)	ΔV_e (m/s)	$\Delta\epsilon_v$ (deg)	$\Delta\alpha_v$ (deg)	$\Delta\psi$ (deg)	$\Delta\lambda$ (deg)
Total 1σ Values Only	422	-2.1	0.012	0.023	-0.010	-0.012
Initial Platform Misalign.:						
(13.62) δ_X	434	-2.2	0.013	0.067	-0.044	-0.018
(29.60) δ_Y	446	-2.1	0.013	0.301	-0.081	-0.025
(14.55) δ_Z	3419	-12.8	0.082	0.0	-0.003	-0.062
Constant Gyro Drift:						
(143.79) $\dot{\delta}_X$	432	-2.4	0.014	0.009	-0.043	-0.018
(248.01) $\dot{\delta}_Y$	456	-2.0	0.014	0.914	-0.159	-0.039
(139.88) $\dot{\delta}_Z$	9738	-19.8	0.483	-0.006	-0.001	-0.075
"g" - Dep. Gyro Drift:						
(654.55) $\dot{\delta}_X/\ddot{X}$	431	-2.5	0.013	-0.064	-0.043	-0.018
(176.81) $\dot{\delta}_X/\ddot{Y}$	431	-2.3	0.013	-0.062	-0.045	-0.018
(903.95) $\dot{\delta}_Y/\ddot{X}$	449	-2.0	0.012	1.344	-0.208	-0.049
(287.57) $\dot{\delta}_Y/\ddot{Y}$	452	-2.1	0.014	0.413	-0.103	-0.029
(578.96) $\dot{\delta}_Z/\ddot{X}$	15057	-24.4	0.842	-0.011	0.000	-0.086
(167.98) $\dot{\delta}_Z/\ddot{Y}$	6138	-16.3	0.202	-0.002	-0.003	-0.066
"g^2" - Dep. Gyro Drift:						
(806.00) $\dot{\delta}_X/\ddot{X}2$	424	-2.5	0.015	-0.051	-0.046	-0.018
(156.90) $\dot{\delta}_X/\ddot{Y}2$	430	-2.3	0.013	0.058	-0.045	-0.018
(1030.96) $\dot{\delta}_Y/\ddot{X}2$	453	-2.0	0.013	1.194	-0.193	-0.046
(239.16) $\dot{\delta}_Y/\ddot{Y}2$	452	-2.1	0.014	0.445	-0.107	-0.029
(687.81) $\dot{\delta}_Z/\ddot{X}2$	14504	-24.4	0.777	-0.011	0.0	-0.085
(145.08) $\dot{\delta}_Z/\ddot{Y}2$	6726	-16.3	0.233	-0.002	-0.003	-0.067
Accelerometer Nonorthog.:						
(2.73) $\delta_{\eta\zeta}$	329	-1.8	0.017	0.023	-0.010	-0.013
(14.55) $\delta_{\xi\zeta}$	4239	-16.8	0.067	0.002	-0.004	-0.060
(16.63) $\delta_{\xi\eta}$	440	-2.2	0.013	0.034	-0.039	-0.017
Accelerometer Scale Factor:						
(2.42) C $\ddot{\xi}$	90	-2.7	0.003	0.023	-0.010	-0.014
(51.30) C $\ddot{\eta}$	1682	8.3	-0.036	0.017	-0.009	-0.024

Note: (1) $\dot{\delta}_i/k$ represents drift about the i-axis proportional to acceleration in k direction.

(2) Errors of such magnitude as used in most of these computations are not to be expected of the guidance systems to be employed on the Saturn flights.

where: C is an (m by n) matrix of partial derivatives relating the parameter errors to each guidance error source.
U is an (n by n) covariance matrix of the guidance error sources which is diagonal with each element the square of the individual error source assumed.

The correlation coefficient between the various parameters, shown in Table V, were obtained from the following equation:

$$\rho ij = \frac{\sigma_{ij}}{\sigma_i \sigma_j} \quad , \text{when } i = j$$

where: σ represents the elements or variances of the N matrix, i refers to the ith row, and j referes to the jth column.

Correlation is relatively high between:

1. Velocity vector and longitude
2. Local azimuth and latitude
3. Radial distance and local elevation angle

TABLE V

CORRELATION COEFFICIENTS

$$\rho_{ij} = \frac{\sigma_{ij}}{\sigma_i \sigma_j}$$

	R_j	V_{ej}	ϵ_{vj}	α_{vj}	ψ_j	λ_j
R_i	1	-.6521	.8399	-.1205	.0839	-.7847
V_{ei}	-.6521	1	-.3989	.1394	-.1258	.9054
ϵ_{vi}	.8399	-.3989	1	-.0916	.0554	-.6131
α_{vi}	-.1205	.1394	-.0916	1	-.8839	-.0029
ψ_i	.0839	-.1258	.0554	-.8839	1	.0435
λ_i	-.7847	.9054	-.6131	-.0029	.0435	1

APPENDIX B

1. Coordinate Systems Defined

a. Earth-fixed Plumbline Coordinates

The earth-fixed plumbline coordinate system is defined as a right-handed Cartesian system with the origin at the launch site, the positive X-axis is directed downrange in the firing direction, the positive Y-axis is normal to the X-Y plane of the origin completing a right-handed system. The coordinates are designated X_e, Y_e, Z_e or in matrix symbol $[X_e]$.

b. Earth-fixed Center-of-Earth Plumbline Coordinates

The origin of the earth-fixed plumbline system translated to the center of the earth defines an earth-fixed, center-of-earth coordinate system. The coordinates are designated X_{ec}, Y_{ec}, Z_{ec} or in matrix symbol $[X_{ec}]$.

c. Space-fixed Plumbline Coordinates

The space-fixed coordinate system is identical with the earth-fixed plumbline system at the instant of launch with the origin remaining as a point fixed in space. The coordinates are designated X_s, Y_s, Z_s or in matrix symbol $[X_s]$.

d. Space-fixed Center-of-Earth Plumbline Coordinates

The origin of the space-fixed coordinate system translated to the center of the earth defines a space-fixed center-of-earth system. The coordinates are designated X_{sc}, Y_{sc}, Z_{sc} or in matrix symbol $[X_{sc}]$.

e. Inertial Reference Coordinates

The inertial reference element is aligned along a set of right-handed Cartesian coordinate axes coinciding with the space-fixed system. The origin is a point of the launch site fixed in space. The movement of the reference element about this set of axes together with accelerometer errors constitute the sources of the guidance intelligence errors. Measurements made in the inertial system do not include the effects of gravity. The matrix symbol for the inertial coordinates is $[X_m]$.

f. Guidance Coordinates

The guidance coordinate system corresponds to the inertial reference system rotated through an angle δ about the X_m-axis and through an angle ϵ about the Z_m-axis. Guidance measurements made in this system may include any desired preset or programmed values entered into the guidance computers. The guidance coordinates are designated ξ, η, ζ and in matrix symbol $[\xi]$.

2. Transformation Formulae

$$[X_{ec}] = [X_e] + [r_o] \quad ; \quad [X_{sc}] = [X_s] + [r_o]$$

where: r_o = radius of earth at launch site

$$[r_o] = \begin{vmatrix} -r_o \cos K \sin \beta \\ r_o \cos \beta \\ r_o \sin K \sin \beta \end{vmatrix}$$

K = firing direction measured clockwise from North

$\beta = \varphi_o - \psi_o$

φ_o = geodetic latitude of launch site

ψ_o = geocentric latitude of launch site

The transformation matricies are

$$[K] = \begin{vmatrix} -\sin K & 0 & -\cos K \\ 0 & 1 & 0 \\ \cos K & 0 & -\sin K \end{vmatrix} \quad ; \quad [K]^T = \begin{vmatrix} -\sin K & 0 & \cos K \\ 0 & 1 & 0 \\ -\cos K & 0 & -\sin K \end{vmatrix}$$

$$[\varphi] = \begin{vmatrix} 1 & 0 & 0 \\ 0 & \cos\varphi_o & -\sin\varphi_o \\ 0 & \sin\varphi_o & \cos\varphi_o \end{vmatrix} ; \quad [\varphi]^T = \begin{vmatrix} 1 & 0 & 0 \\ 0 & \cos\varphi_o & \sin\varphi_o \\ 0 & -\sin\varphi_o & \cos\varphi_o \end{vmatrix}$$

$$[\omega t] = \begin{vmatrix} \cos\omega t & -\sin\omega t & 0 \\ \sin\omega t & \cos\omega t & 0 \\ 0 & 0 & 1 \end{vmatrix} ; \quad [\omega t]^T = \begin{vmatrix} \cos\omega t & \sin\omega t & 0 \\ -\sin\omega t & \cos\omega t & 0 \\ 0 & 0 & 1 \end{vmatrix}$$

$$[\dot{\omega} t] = \begin{vmatrix} -\omega\sin\omega t & -\omega\cos\omega t & 0 \\ \omega\cos\omega t & -\omega\sin\omega t & 0 \\ 0 & 0 & 0 \end{vmatrix} ; \quad [\dot{\omega} t]^T = \begin{vmatrix} -\omega\sin\omega t & \omega\cos\omega t & 0 \\ -\omega\cos\omega t & -\omega\sin\omega t & 0 \\ 0 & 0 & 0 \end{vmatrix}$$

$$[\ddot{\omega} t] = \begin{vmatrix} -\omega^2\cos\omega t & \omega^2\sin\omega t & 0 \\ -\omega^2\sin\omega t & -\omega^2\cos\omega t & 0 \\ 0 & 0 & 0 \end{vmatrix} ; \quad [\ddot{\omega} t]^T = \begin{vmatrix} -\omega^2\cos\omega t & -\omega^2\sin\omega t & 0 \\ \omega^2\sin\omega t & -\omega^2\cos\omega t & 0 \\ 0 & 0 & 0 \end{vmatrix}$$

where: ω = angular velocity of earth rotation
t = time from liftoff ($t_n - t_o$)

Let:

$$[T] = [K]^T [\varphi]^T [\omega t] [\varphi] [K] ; \quad [T]^T = [K]^T [\varphi]^T [\omega t]^T [\varphi] [K]$$

$$[\dot{T}] = [K]^T [\varphi]^T [\dot{\omega} t] [\varphi] [K] ; \quad [\dot{T}]^T = [K]^T [\varphi]^T [\dot{\omega} t]^T [\varphi] [K]$$

$$[\ddot{T}] = [K]^T [\varphi]^T [\ddot{\omega} t] [\varphi] [K] ; \quad [\ddot{T}]^T = [K]^T [\varphi]^T [\ddot{\omega} t]^T [\varphi] [K]$$

Then:

$$(1.01)\quad [\ddot{X}_s] = [T]\,[\ddot{X}_e] + 2\,[\dot{T}][X_e] + [\ddot{T}][X_{ec}]\ ;\ [\ddot{X}_e] = [T]^T\,[\ddot{X}_s] + 2\,[\dot{T}]^T\,[\dot{X}_s] + [\ddot{T}]^T\,[X_{sc}]$$

$$(1.02)\quad [\dot{X}_s] = [T]\,[\dot{X}_e] + [\dot{T}][X_{ec}]\ ;\ [\dot{X}_e] = [T]^T\,[\dot{X}_s] + [\dot{T}]^T\,[X_{sc}]$$

$$(1.03)\quad [X_s] = [T]\,[X_{ec}] - [r_o]\ ;\ [X_e] = [T]^T\,[X_{sc}] - [r_o]$$

Equations 1.01, 1.02, and 1.03 transform the earth-fixed components to corresponding space-fixed values.

The inertial measurements are made as if the earth was fixed in space and there were no gravitational effects on the vehicle.

$$(1.04)\quad [\ddot{X}_m] = [\ddot{X}_s] - [\ddot{X}_g]$$

$$(1.05)\quad [\dot{X}_m] = [\dot{X}_s] - [\dot{X}_g] - [\dot{X}_{so}]$$

$$(1.06)\quad [X_m] = [X_s] - [X_g] - [t]\,[\dot{X}_o] - [X_{so}]$$

By substituting equations 1.01, 1.02, 1.03 into 1.04, 1.05, and 1.06 respectively

$$(1.07)\quad [\ddot{X}_m] = [T]\,[\ddot{X}_e] + 2\,[\dot{T}]\,[\dot{X}_e] + [\ddot{T}]\,[X_{ec}] - [\ddot{X}_g]$$

$$(1.08)\quad [\dot{X}_m] = [T]\,[\dot{X}_e] + [\dot{T}]\,[X_{ec}] - [\dot{X}_g] - [\dot{X}_{so}]$$

$$(1.09)\quad [X_m] = [T]\,[X_{ec}] - [r_o] - [X_g] - [t]\,[\dot{X}_o] - [X_{so}]$$

where: $[X_g]$ = gravitational components along the X, Y, Z axes

$[X_{so}]$ = initial space-fixed components

$$[t] \text{ is a diagonal matrix} \quad \begin{vmatrix} t & 0 & 0 \\ 0 & t & 0 \\ 0 & 0 & t \end{vmatrix}$$

The inertial guidance measurements are made in a system rotated from the $[X_m]$ coordinate system through the angles δ about the X-axis and ϵ about the Z-axis. The rotations given are counterclockwise.

$$[\delta] = \begin{vmatrix} 1 & 0 & 0 \\ 0 & \cos\delta & \sin\delta \\ 0 & -\sin\delta & \cos\delta \end{vmatrix} ; \quad [\epsilon] = \begin{vmatrix} \cos\epsilon & \sin\epsilon & 0 \\ -\sin\epsilon & \cos\epsilon & 0 \\ 0 & 0 & 1 \end{vmatrix}$$

Let: $[P] = [\epsilon][\delta]$ and $[P]^T = [\epsilon]^T [\delta]^T$

Then:

(1.10) $[\ddot{\xi}] = [P] [\ddot{X}_m]$

(1.11) $[\dot{\xi}] = [P] [\dot{X}_m]$

(1.12) $[\xi] = [P] [X_m]$

By substituting equations 1.07, 1.08, and 1.09 into 1.10, 1.11, and 1.12, respectively

(1.13) $[\ddot{\xi}] = [P] [T] [\ddot{X}_e] + 2 [\dot{T}] [\dot{X}_e] + [\ddot{T}][X_{ec}] - [\ddot{X}_g]$

(1.14) $[\dot{\xi}] = [P] [T] [\dot{X}_e] + [\dot{T}] [X_{ec}] - [\dot{X}_{so}] - [\dot{X}_g]$

(1.15) $[\xi] = [P] [T] [X_{ec}] - [r_o] - [t] [\dot{X}_{so}] - [X_{so}] - [X_g]$

The guidance measurements may include preset and/or programmed values.

Let: S = preset slant range displacement

Q = preset slant range velocity

$\dot{\eta}_p$ = preset slant altitude velocity

η_p = preset slant altitude displacement

$\bar{\dot{\eta}}$ = programmed slant altitude velocity

$$\bar{\eta} = \int_{t=0}^{t} \bar{\dot{\eta}}\, dt$$

$$[Q] = \begin{matrix} Q \\ \dot{\eta}_p + \bar{\dot{\eta}} \\ 0 \end{matrix}$$

$$[S] = \begin{vmatrix} S + Qt \\ \eta_p + \bar{\eta} \\ 0 \end{vmatrix}$$

Then equations 1.14 and 1.15 become

$$(1.16)\quad [\dot{\xi}_i] = [P]\,[T]\,[\dot{X}_e] + [\dot{T}]\,[X_{ec}] - [\dot{X}_{so}] - [\dot{X}_g] + [Q]$$

$$(1.17)\quad [\xi_i] = [P]\,[T]\,[X_{ec}] - [r_o] - [t]\,[X_{so}] - [X_{so}] - [X_g] + [S]$$

Equations 1.13, 1.14, 1.15 or equations 1.13, 1.16, 1.17 would transform earth-fixed tracking data into inertial guidance measurements corresponding to the outputs of the guidance accelerometers and computers.

The inertial guidance measurements may be transformed into earth-fixed components.

$$(1.18)\quad [\ddot{X}_e] = [T]^T \left\{ [P]^T \left([\ddot{\xi}] + [\ddot{\xi}_g] \right) \right\} +$$

$$2\,[\dot{T}]^T \left\{ [P]^T \left([\dot{\xi}_i] - [Q] + [\dot{\xi}_{so}] + [\dot{\xi}_g] \right) \right\} +$$

$$[\ddot{T}]^T \left\{ [P]^T \left([\xi_i] - [S] + [t][\dot{\xi}_{so}] + [\xi_{so}][\xi_g] \right) + [r_o] \right\}$$

$$(1.19)\quad [\dot{X}_e] = [T]^T \left\{ [P]^T \left([\dot{\xi}_i] - [Q] + [\dot{\xi}_{so}] + [\dot{\xi}_g] \right) \right\} +$$

$$[\dot{T}]^T \left\{ [P]^T \left([\xi_i] - [S] + [t]\,[\dot{\xi}_{so}] + [\xi_{so}] + [\xi_g] \right) + [r_o] \right\}$$

$$(1.20)\quad [X_e] = [T]^T \left\{ [P]^T \left([\xi_i] - [S] + [t]\,[\dot{\xi}_{so}] + [\xi_{so}] + [\xi_g] \right) + [r_o] \right\} - [r_o]$$

where: $[\dot{\xi}_{so}] = [P]\,[\dot{X}_{so}]$

and: $[\xi_{so}] = [P]\,[X_{so}]$

The gravitational components are more difficult to determine from inertial measurements than from earth-fixed positions. The gravitational accelerations are functions of positions with respect to the earth's center and

$$[\dot{X}_g] = \int_{t=0}^{t} [\ddot{X}_g]\, dt$$

$$[X_g] = \int_{t=0}^{t} [\ddot{X}_g]\, dt^2$$

The following equations are of sufficient accuracy in most cases and simplify the work necessary for equations 1.18, 1.19, 1.20. The gravitational components are determine from external tracking data.

$$(1.21)\quad [\ddot{X}_e] = [T]^T\{[P]^T([\ddot{\xi}] + [\ddot{X}_g])\} +$$

$$2\,[\dot{T}]^T\{[P]^T([\dot{\xi}_i] - [Q]) + [\dot{X}_{so}] + [\dot{X}_g]\} +$$

$$[\ddot{T}]^T\{[P]^T([\xi_i] - [S]) + [t]\,[\dot{X}_{so}] + [X_g] + [r_o]\}$$

$$(1.22)\quad [\dot{X}_e] = [T]^T\{[P]^T([\dot{\xi}_i] - [Q]) + [\dot{X}_{so}] + [\dot{X}_g]\} +$$

$$[\dot{T}]^T\{[P]^T([\xi_i] - [S]) + [t]\,[\dot{X}_{so}] + [X_{so}] + [X_g] + [r_o]\}$$

$$(1.23)\quad [X_e] = [T]^T\{[P]^T([\xi_i] - [S]) + [t]\,[\dot{X}_{so}] + [X_{so}] + [X_g] + [r_o]\} - [r_o]$$

APPENDIX C

DEVELOPMENT OF EQUATIONS FOR GUIDANCE ERRORS

1. Nonorthogonal accelerometer axes (measuring directions)

We shall first consider $\ddot{\xi}$ nonorthogonal with respect to the $\ddot{\eta}$ and $\ddot{\zeta}$ axes:

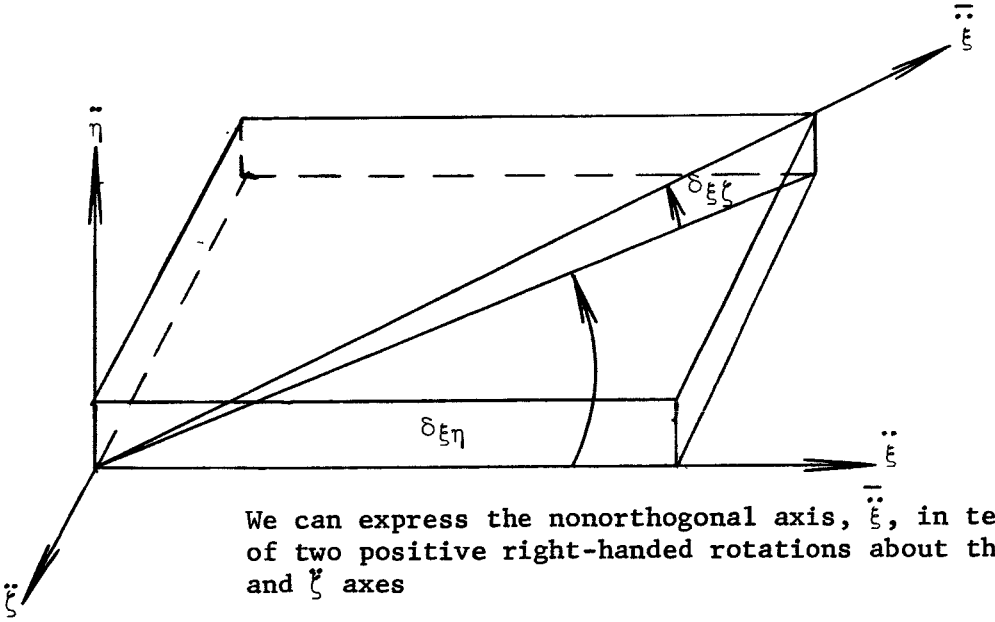

We can express the nonorthogonal axis, $\bar{\ddot{\xi}}$, in terms of two positive right-handed rotations about the $\ddot{\eta}$ and $\ddot{\zeta}$ axes

$$\begin{vmatrix} \bar{\ddot{\xi}} \\ 0 \\ 0 \end{vmatrix} = \begin{vmatrix} \cos\delta_{\xi\zeta} & \sin\delta_{\xi\zeta} & 0 \\ -\sin\delta_{\xi\zeta} & \cos\delta_{\xi\zeta} & 0 \\ 0 & 0 & 1 \end{vmatrix} \begin{vmatrix} \cos\delta_{\xi\eta} & 0 & -\sin\delta_{\xi\eta} \\ 0 & 1 & 0 \\ \sin\delta_{\xi\eta} & 0 & \cos\delta_{\xi\eta} \end{vmatrix} \begin{vmatrix} \ddot{\xi} \\ \ddot{\eta} \\ \ddot{\zeta} \end{vmatrix}$$

$$(2.01)\quad \bar{\ddot{\xi}} = \cos\delta_{\xi\zeta}\cos\delta_{\xi\eta}\ddot{\xi} + \sin\delta_{\xi\zeta}\ddot{\eta} - \cos\delta_{\xi\zeta}\sin\delta_{\xi\eta}\ddot{\zeta}$$

2. Next let us consider $\ddot{\eta}$ nonorthogonal with respect to the $\ddot{\xi}$ and $\ddot{\zeta}$ axes.

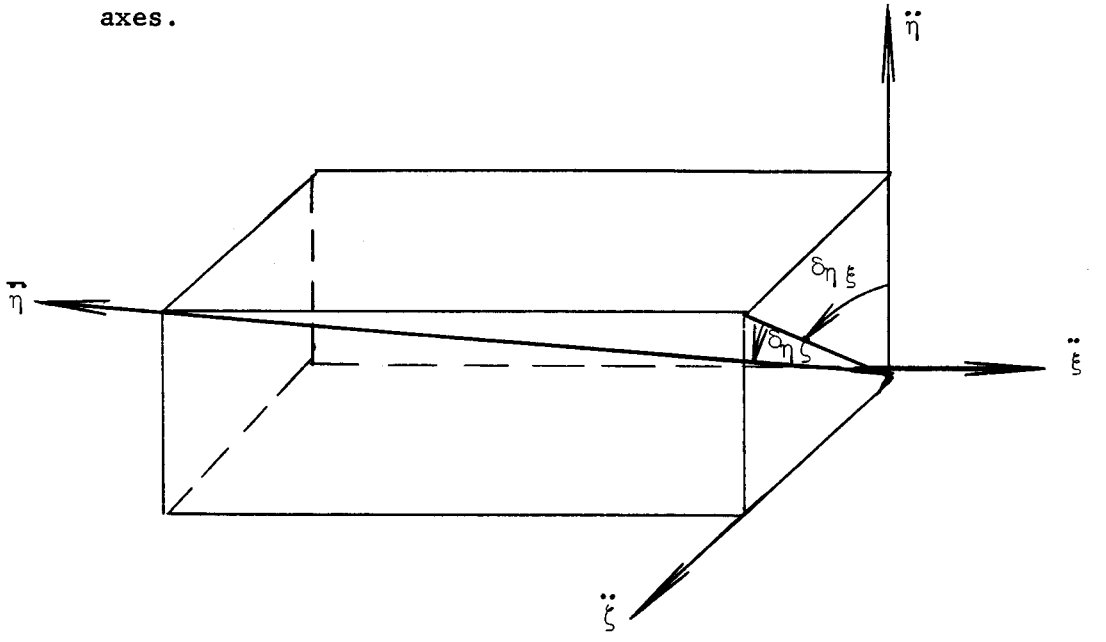

We can express the nonorthogonal axis $\ddot{\eta}$ in terms of two positive right-handed rotations about the $\ddot{\xi}$ and $\ddot{\zeta}$ axes.

$$\begin{vmatrix} 0 \\ \bar{\ddot{\eta}} \\ 0 \end{vmatrix} = \begin{vmatrix} \cos\delta_{\eta\zeta} & \sin\delta_{\eta\zeta} & 0 \\ -\sin\delta_{\eta\zeta} & \cos\delta_{\eta\zeta} & 0 \\ 0 & 0 & 1 \end{vmatrix} \begin{vmatrix} 1 & 0 & 0 \\ 0 & \cos\delta_{\eta\xi} & \sin\delta_{\eta\xi} \\ 0 & -\sin\delta_{\eta\xi} & \cos\delta_{\eta\xi} \end{vmatrix} \begin{vmatrix} \ddot{\xi} \\ \ddot{\eta} \\ \ddot{\zeta} \end{vmatrix}$$

$$(2.02)\quad \bar{\ddot{\eta}} = -\sin\delta_{\eta\zeta}\ddot{\xi} + \cos\delta_{\eta\zeta}\cos\delta_{\eta\xi}\ddot{\eta} + \cos\delta_{\eta\zeta}\sin\delta_{\eta\xi}\ddot{\zeta}$$

3. Finally we shall consider $\ddot{\zeta}$ nonorthogonal with respect to the $\ddot{\xi}$ and $\ddot{\eta}$ axes.

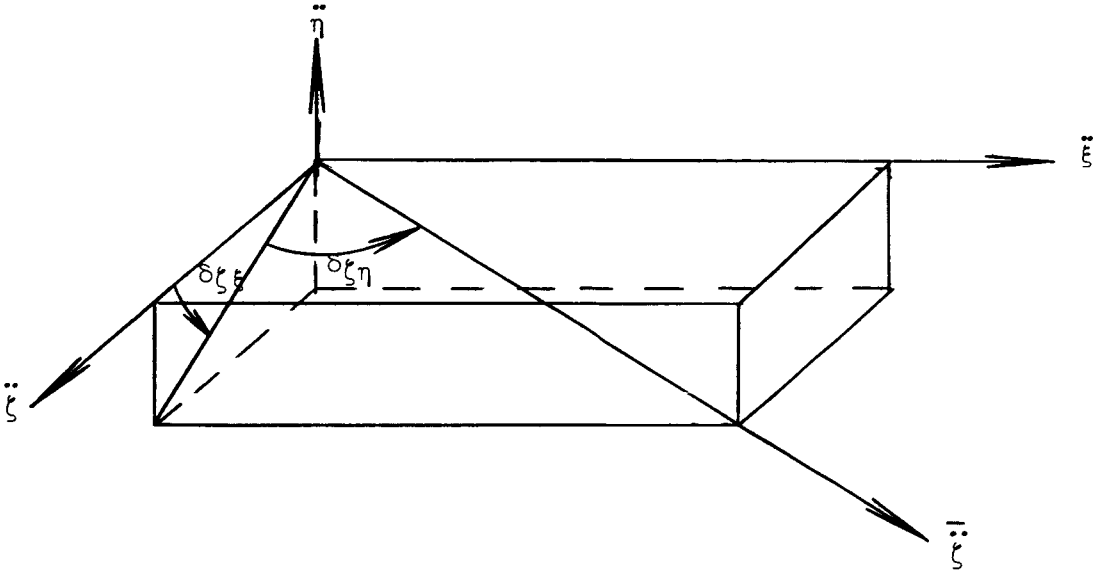

We can express the nonorthogonal $\ddot{\zeta}$ axis in terms of two positive right-handed rotations about the $\ddot{\xi}$ and $\ddot{\eta}$ axes.

$$\begin{vmatrix} 0 \\ 0 \\ \bar{\ddot{\zeta}} \end{vmatrix} = \begin{vmatrix} \cos\delta_{\zeta\eta} & 0 & -\sin\delta_{\zeta\eta} \\ 0 & 1 & 0 \\ \sin\delta_{\zeta\eta} & 0 & \cos\delta_{\zeta\eta} \end{vmatrix} \begin{vmatrix} 1 & 0 & 0 \\ 0 & \cos\delta_{\zeta\xi} & \sin\delta_{\zeta\xi} \\ 0 & -\sin\delta_{\zeta\xi} & \sin\delta_{\zeta\xi} \end{vmatrix} \begin{vmatrix} \ddot{\xi} \\ \ddot{\eta} \\ \ddot{\zeta} \end{vmatrix}$$

$$(2.03)\quad \bar{\ddot{\zeta}} = \sin\delta_{\zeta\eta}\ddot{\xi} - \cos\delta_{\zeta\eta}\sin\delta_{\zeta\xi}\ddot{\eta} + \cos\delta_{\zeta\eta}\cos\delta_{\zeta\xi}\ddot{\zeta}$$

We can now express the three mutually nonorthogonal axes $\bar{\ddot{\xi}}$, $\bar{\ddot{\eta}}$, $\bar{\ddot{\zeta}}$ with respect to the three mutually orthogonal axes $\ddot{\xi}$, $\ddot{\eta}$, $\ddot{\zeta}$

$$(2.04)\quad \begin{vmatrix} \ddot{\bar{\xi}} \\ \ddot{\bar{\eta}} \\ \ddot{\bar{\zeta}} \end{vmatrix} = \begin{vmatrix} \cos\delta_{\xi\zeta}\cos\delta_{\xi\eta} & \sin\delta_{\xi\zeta} & -\cos\delta_{\xi\zeta}\sin\delta_{\xi\eta} \\ -\sin\delta_{\eta\zeta} & \cos\delta_{\eta\zeta}\cos\delta_{\eta\xi} & \cos\delta_{\eta\zeta}\sin\delta_{\eta\xi} \\ \sin\delta_{\zeta\eta} & -\cos\delta_{\zeta\eta}\sin\delta_{\zeta\xi} & \cos\delta_{\zeta\eta}\cos\zeta\xi \end{vmatrix} \begin{vmatrix} \ddot{\xi} \\ \ddot{\eta} \\ \ddot{\zeta} \end{vmatrix}$$

in symbolic notation $[\ddot{\bar{\xi}}] = [C_\delta]\,[\ddot{\xi}]$

4. Consider the case when we have the platform misalignments δ_x, δ_y, δ_z along XXXM, YYYM, ZZZM axes, respectively. This misalignment can be expressed as the product of three matrices.

$$\begin{vmatrix} \delta_{11} & \delta_{12} & \delta_{13} \\ \delta_{21} & \delta_{22} & \delta_{23} \\ \delta_{31} & \delta_{32} & \delta_{33} \end{vmatrix} = \begin{vmatrix} \cos\delta_z & \sin\delta_z & 0 \\ -\sin\delta_z & \cos\delta_z & 0 \\ 0 & 0 & 1 \end{vmatrix} \begin{vmatrix} \cos\delta_y & 0 & -\sin\delta_y \\ 0 & 1 & 0 \\ \sin\delta_y & 0 & \cos\delta_y \end{vmatrix}$$

$$(2.05)\qquad \begin{vmatrix} 1 & 0 & 0 \\ 0 & \cos\delta_x & \sin\delta_x \\ 0 & -\sin\delta_x & \cos\delta_x \end{vmatrix}$$

where

$$\delta_{11} = \cos\delta_z\cos\delta_y \qquad \delta_{12} = \cos\delta_z\sin\delta_y\sin\delta_x + \sin\delta_x\cos\delta_x$$

$$\delta_{21} = -\sin\delta_z\cos\delta_y \qquad \delta_{22} = \cos\delta_z\cos\delta_x - \sin\delta_z\sin\delta_y\sin\delta_x$$

$$\delta_{31} = \sin\delta_y \qquad \delta_{32} = -\cos\delta_y\sin\delta_x$$

$$(2.06)\qquad \delta_{13} = \sin\delta_z\sin\delta_x - \cos\delta_z\sin\delta_y\cos\delta_x$$

$$\delta_{23} = \cos\delta_z\sin\delta_x + \sin\delta_z\sin\delta_y\cos\delta_x$$

$$\delta_{33} = \cos\delta_y\cos\delta_x\,,$$

where:

$$\delta_x = \delta_{x_o} + \int \delta_x dt \quad ; \quad \delta_y = \delta_{y_o} + \int \delta_y dt \quad ; \quad \delta_z = \delta_{z_o} + \int \delta_z dt \, .$$

We can write δ_x, δ_y, δ_z as follows:

$$\begin{vmatrix} \delta_x \\ \delta_y \\ \delta_z \end{vmatrix} = \begin{vmatrix} 1/\cos \delta_y & 0 & 0 \\ 0 & 1/\cos \delta_y & 0 \\ 0 & 0 & 1/\cos \delta_y \end{vmatrix}$$

(2.07)

$$\begin{vmatrix} \cos \delta_z & -\sin \delta_z & 0 \\ \cos \delta_y \sin \delta_z & \cos \delta_y \cos \delta_z & 0 \\ -\sin \delta_y \cos \delta_z & \sin \delta_y \sin \delta_z & \cos \delta_y \end{vmatrix} \begin{vmatrix} u_1 \\ u_2 \\ u_3 \end{vmatrix}$$

5. We can write u_1, u_2, u_3 as follows:

$$\begin{vmatrix} u_1 \\ u_2 \\ u_3 \end{vmatrix} = \begin{vmatrix} u_{10} \\ u_{20} \\ u_{30} \end{vmatrix} + \begin{vmatrix} T & 0 & 0 \\ 0 & T & 0 \\ 0 & 0 & T \end{vmatrix} \begin{vmatrix} \dot{u}_{10} \\ \dot{u}_{20} \\ \dot{u}_{30} \end{vmatrix} + \begin{vmatrix} K_{11} & K_{12} & K_{13} \\ K_{21} & K_{22} & K_{23} \\ K_{31} & K_{32} & K_{33} \end{vmatrix} \begin{vmatrix} DDXM \\ DDYM \\ DDZM \end{vmatrix} +$$

(2.08)

$$\begin{vmatrix} H_{11} & H_{12} & H_{13} \\ H_{21} & H_{22} & H_{23} \\ H_{31} & H_{32} & H_{33} \end{vmatrix} \begin{vmatrix} \overline{DDXM}^2 \\ \overline{DDYM}^2 \\ \overline{DDZM}^2 \end{vmatrix}$$

Therefore, we can define u_1, u_2, and u_3 at any time T. Having determined these quantities, we can substitute into the matrices defining $\dot{\delta}_x$, $\dot{\delta}_y$, $\dot{\delta}_z$. Integrating $\dot{\delta}_x$, $\dot{\delta}_y$, $\dot{\delta}_z$ numerically we can define δ_x, δ_y and δ_z at any time T.

We shall now express a relationship between the misaligned platform axes (XXXM', YYYM', ZZZM') and the initial platform axes (XXXM, YYYM, ZZZM) in terms of accelerations,

$$(2.09)\quad \begin{vmatrix} DDXM' \\ DDYM' \\ DDZM' \end{vmatrix} = \begin{vmatrix} \delta_{11} & \delta_{12} & \delta_{13} \\ \delta_{21} & \delta_{22} & \delta_{23} \\ \delta_{31} & \delta_{32} & \delta_{33} \end{vmatrix} \begin{vmatrix} DDXM \\ DDYM \\ DDZM \end{vmatrix} \quad \text{or} \quad [\ddot{X}_m'] = [\delta]\,[\ddot{X}_m]$$

or expressing the above in terms of accelerometer output:

$$(2.10)\quad \begin{vmatrix} \ddot{\xi}' \\ \ddot{\eta}' \\ \ddot{\zeta}' \end{vmatrix} = \begin{vmatrix} \cos\epsilon & \sin\epsilon & 0 \\ -\sin\epsilon & \cos\epsilon & 0 \\ 0 & 0 & 1 \end{vmatrix} \begin{vmatrix} \delta_{11} & \delta_{12} & \delta_{13} \\ \delta_{21} & \delta_{22} & \delta_{23} \\ \delta_{31} & \delta_{32} & \delta_{33} \end{vmatrix} \begin{vmatrix} DDXM \\ DDYM \\ DDZM \end{vmatrix}$$

or $[\ddot{\xi}'] = [\epsilon]\,[\delta]\,[\ddot{X}_m]$

6. With equation (2.10) we have considered the effect of platform deviation on accelerometer output. With equation (2.04) we have considered the effect nonorthogonal accelerometer axes have on accelerometer output. We can now express the effect on accelerometer output due to platform misalignments and also due to nonorthogonal accelerometer axes as follows:

$$\begin{vmatrix} \ddot{\xi}'' \\ \ddot{\eta}'' \\ \ddot{\zeta}'' \end{vmatrix} = \begin{vmatrix} \cos\delta_{\xi\zeta}\cos\delta_{\xi\eta} & \sin\delta_{\xi\zeta} & -\cos\delta_{\xi\zeta}\sin\delta_{\xi\eta} \\ -\sin\delta_{\eta\zeta} & \cos\delta_{\eta\zeta}\cos\delta_{\eta\xi} & \cos\delta_{\eta\zeta}\sin\delta_{\eta\xi} \\ \sin\delta_{\zeta\eta} & -\cos\delta_{\zeta\eta}\sin\delta_{\zeta\xi} & \cos\delta_{\zeta\eta}\cos\delta_{\zeta\xi} \end{vmatrix}$$

(2.11)

$$\begin{vmatrix} \cos\epsilon & \sin\epsilon & 0 \\ -\sin\epsilon & \cos\epsilon & 0 \\ 0 & 0 & 1 \end{vmatrix} \begin{vmatrix} \delta_{11} & \delta_{12} & \delta_{13} \\ \delta_{21} & \delta_{22} & \delta_{23} \\ \delta_{31} & \delta_{32} & \delta_{33} \end{vmatrix} \begin{vmatrix} DDXM \\ DDYM \\ DDZM \end{vmatrix}$$

(2.12) or $[\ddot{\xi}''] = [C_\delta]\,[\epsilon]\,[\delta]\,[\ddot{X}_m]$.

The accelerometer output is also affected by a scale factor Q which is denoted by the diagonal matrix [Q] .

(2.13) $$[Q] = \begin{vmatrix} Q_{11} & 0 & 0 \\ 0 & Q_{12} & 0 \\ 0 & 0 & Q_{33} \end{vmatrix}$$

Therefore, we can now write the accelerometer output as affected by nonorthogonality of the accelerometer axes, misaligned platform axes, and scale factor error:

(2.14) $$[\ddot{\xi}''] = [Q]\,[C_\delta]\,[\epsilon]\,[\delta]\,[\ddot{X}_m] = [Q]\,[C_\delta]\,[\epsilon]\,[\ddot{X}'_m] = [\Omega]\,[\ddot{X}'_m]$$

where $[\Omega] = [Q]\,[C_\delta]\,[\epsilon]$.

7. If $[Q]$, $[C_{\delta}]$, $[\epsilon]$ are constants as an integration option we can integrate $[\ddot{X}_m']$ and then solve for $[\dot{\xi}']$ and $[\xi']$ as follows:

$$(2.15)\quad [\dot{\xi}''] = [\Omega]\ [\ddot{X}_m']\ dt + [\dot{\xi}_o] \text{ where } [\dot{\xi}_o] = \begin{vmatrix} \dot{\xi}_o \\ \dot{\eta}_o \\ \dot{\zeta}_o \end{vmatrix} = \text{preset values}$$

$$(2.16)\quad [\xi''] = [\Omega]\ [\dot{X}_m']\ dt + [\dot{\xi}_o]\ [T] + [\xi_o]$$

$$\text{where } T = \begin{vmatrix} T & 0 & 0 \\ 0 & T & 0 \\ 0 & 0 & T \end{vmatrix};\ [\dot{\xi}_o] = \begin{vmatrix} \dot{\xi}_o \\ \dot{\eta}_o \\ \dot{\zeta}_o \end{vmatrix};\ [\xi_o] = \begin{vmatrix} \xi_o \\ \eta_o \\ \zeta_o \end{vmatrix} \quad \begin{matrix} \text{Guidance} \\ \text{Computer} \\ \text{Presettings} \end{matrix}$$

However, if $[\Omega]$ is not constant we must integrate $[\ddot{\xi}']$ to obtain and $[\dot{\xi}']$ and $[\xi']$

$$(2.17)\quad \text{i.e.,}\ [\dot{\xi}'] = \int [\ddot{\xi}']\ dt + [\dot{\xi}_o]$$

$$(2.18)\quad [\xi'] = \int [\dot{\xi}']\ dt + [\dot{\xi}_o]\ [T] + [\xi_o].$$

It must be remembered that we must integrate both $[\dddot{X}_m']$ and $[\ddot{\xi}']$ when $[\Omega]$ is not a constant because the integrated $[\ddot{X}_m']$ output is needed for conversion to space-fixed (w/gravity) quantities.

APPENDIX D

1. Transformation From Earth-Fixed Plumbline System to Earth-Fixed Ephemeris Coordinate System

This section is primarily concerned with the transformation from guidance coordinates to the ephemeris coordinate system. However, to eliminate repetition of defining terms the transformation from the earth-fixed (launch site origin) to the ephemeris earth-fixed system is first presented. The ephemeris coordinate system is defined in Appendix A.

$[X_e']$ = earth-fixed coordinates in ephemeris system

$[\dot{X}_e']$ = earth-fixed velocities in ephemeris system

$$(3.01)\quad [X_e'] = [C]\ [B]\ [D]\ [X_{ec}]$$

$$(3.02)\quad [\dot{X}_e'] = [C]\ [B]\ [D]\ [\dot{X}_e]$$

where:

$$[C] = \begin{vmatrix} \sin\lambda_o & \cos\lambda_o & 0 \\ \cos\lambda_o & -\sin\lambda_o & 0 \\ 0 & 0 & 1 \end{vmatrix}$$

$$[B] = \begin{vmatrix} 1 & 0 & 0 \\ 0 & \cos\varphi_o & \sin\varphi_o \\ 0 & \sin\varphi_o & -\cos\varphi_o \end{vmatrix} ; \quad [D] = \begin{vmatrix} \sin K & 0 & \cos K \\ 0 & 1 & 0 \\ -\cos K & 0 & \sin K \end{vmatrix}$$

2. The Transformation from Inertial Guidance Coordinate to Earth-Fixed Ephemeris Coordinates

Positions:

$$[X_e] = [T]^T \left\{ [P]^T \left([\xi_i] - [S] \right) + [t][\dot{X}_{so}] + [X_{so}] + [X_g] + [r_o] \right\} - [r_o]$$

$$[X_e] + [r_o] = [X_{ec}] = [T]^T \left\{ [P]^T \left([\xi_i] - [S] \right) + [t][\dot{X}_{so}] + [X_{so}] + [X_g] + [r_o] \right\}$$

Substituting into equation 3.01

$$(3.03) \quad [X_e'] = [C][B][D][T]^T \left\{ [P]^T \left([\xi_i] - [S] \right) + [t][\dot{X}_{so}] + [X_{so}] + [X_g] + [r_o] \right\}.$$

Velocities:

$$[\dot{X}_e] = [T]^T \left\{ [P]^T \left([\xi_i] - [Q] \right) + [\dot{X}_{so}] + [\dot{X}_g] \right\} +$$

$$[\dot{T}]^T \left\{ [P]^T \left([\xi_i] - [S] \right) + [t][\dot{X}_{so}] + [X_{so}] + [X_g] + [r_o] \right\}.$$

Substituting into equation 3.02

$$[\dot{X}_e'] = [C][B][D][T]^T \left\{ [P]^T \left([\xi_i] - [Q] \right) + [\dot{X}_{so}] + [\dot{X}_g] \right\} +$$

$$(3.04)$$

$$[\dot{T}]^T \left\{ [P]^T \left([\xi_i] - [S] \right) + [t] [\dot{X}_{so}] + [X_{so}] + [X_g] + [r_o] \right\}.$$

3. $R = \sqrt{X_e'^2 + Y_e'^2 + Z_e'^2}$

$$\psi = \tan^{-1}\left(\frac{Z_e'}{\sqrt{X_e'^2 + Y_e'^2}}\right) \qquad -90° \leqq \psi \leqq 90°$$

$$\lambda = \tan^{-1}\left(\frac{Y_e'}{X_e'}\right) \qquad 0° \leqq \lambda \leqq 360°$$

$$V_e = \sqrt{a^2 + b^2 + c^2}$$

$$\epsilon_v = \tan^{-1}\left(\frac{c}{\sqrt{a^2 + b^2}}\right) \qquad -90° \leqq \epsilon_v \leqq 90°$$

$$\alpha_v = \tan^{-1}\left(a/b\right) \qquad 0° \leqq \alpha_v \leqq 360°$$

where

a, b, c are directional cosines of the velocity vector in the geospherical coordinate system. (See Figure 9.)

$$\begin{vmatrix} a \\ b \\ c \end{vmatrix} = \begin{vmatrix} 1 & 0 & 0 \\ 0 & \sin\psi & \cos\psi \\ 0 & -\cos\psi & \sin\psi \end{vmatrix} \begin{vmatrix} -\sin\lambda & \cos\lambda & 0 \\ -\cos\lambda & -\sin\lambda & 0 \\ 0 & 0 & 1 \end{vmatrix} \begin{vmatrix} \dot{X}_e' \\ \dot{Y}_e' \\ \dot{Z}_e' \end{vmatrix}$$

REFERENCES

1. Report No. DA-TN-48-58, A Transformation from an Earth-Fixed Plumbline Coordinate System to the Space-Fixed Satellite Orbit Coordinate System, C. R. Fulmer, July 25, 1958.

2. American Rocket Society Paper, The Path-Adaptive Mode for Guiding Space Flight Vehicles, W. E. Miner and D. H. Schmieder, August 7-9, 1961.

3. American Rocket Society Paper, Saturn Ascending Phase Guidance and Control Techniques, F. Brooks Moore and Melvin Brooks, July 17-19, 1962.

APPROVAL MTP-AERO-62-76

A METHOD OF DETERMINING THE SOURCE OF ERRORS IN GUIDANCE MEASUREMENTS AND RESULTANT ERRORS IN EARTH-FIXED COMPONENTS

By

R. A. Chapman

The information in this report has been reviewed for security classification. Review of any information concerning Department of Defense or Atomic Energy Commission programs has been made by the MSFC Security Classification Officer. This report, in its entirety, has been determined to be unclassified.

C. R. FULMER
Chief, Flight Simulation Section

FRIDTJOF SPEER
Chief, Flight Evaluation Branch

E. D. GEISSLER
Director, Aeroballistics Division

DISTRIBUTION

Dr. von Braun, M-DIR
Dr. Rees, M-DEP-R&D

M-AERO
Dr. Geissler, M-AERO-DIR
Mr. Jean, M-AERO-PS
Mr. Dahm, M-AERO-A
Dr. Speer, M-AERO-F
Mr. Fulmer, M-AERO-F
Mr. Lindberg, M-AERO-F
Mr. Kurtz, M-AERO-F
Mr. Chapman, M-AERO-F (10)
Mr. W. W. Vaughan (2)

M-L&M
Mr. Hueter, M-L&M-DIR

M-COMP
Dr. Hoelzer, M-COMP-DIR
Mr. Moore, M-COMP-R
Mr. Tondera, M-COMP-R
Mr. J. W. Clark, M-COMP-GE

M-ME
Mr. Kuers, M-ME-DIR

M-FPO
Mr. Koelle, M-FPO-DIR

M-ASTR
Dr. Haeussermann, M-ASTR-DIR
Mr. Noel, M-ASTR-TSJ
Mr. Taylor, M-ASTR-R
Mr. Hosenthien, M-ASTR-F
Mr. Mandel, M-ASTR-G
Mr. Moore, M-ASTR-N
Mr. McMahen, M-ASTR-NT
Mr. Gassaway, M-ASTR-NT
Mr. Jenke, M-ASTR-MG

M-LVO
Dr. Debus, M-LVO-DIR
Dr. Gruene, M-LVO-G
Mr. Zeiler, M-LVO-M

M-QUAL
Mr. Grau, M-QUAL-DIR

M-RP
Dr. Stuhlinger, M-RP-DIR

M-SAT
Dr. Lange, M-SAT-DIR

M-P&VE
Mr. Mrazek, M-P&VE-DIR

M-TPC
Mr. Smith, M-TPC

M-TEST
Mr. Heimburg, M-TEST-DIR

M-MS
M-MS-IPL (8)
M-MS-IP
M-MS-H
M-HME-P
M-PAT

DISTRIBUTION (CONT.)

EXTERNAL

Goddard Space Flight Center
4555 Overlook Avenue
Washington 25, D. C.
Attn: Herman LaGow

Manned Spacecraft Center
Houston 1, Texas - P. O. Box 1537
Attn: Director: Robert R. Gilruth

Director, Lewis Research Center: Abe Silverstein
National Aeronautics & Space Administration
21000 Brookpark Road
Cleveland 35, Ohio

Jet Propulsion Lab
4800 Oak Grove Drive
Pasadena 2, California
Attn: Irl Newlan, Reports Group

Douglas Aircraft Company, Inc.
Missile and Space Systems Engineering
Santa Monica, California
Attn: H. M. Thomas
A. J. German

Boeing Corporation
Saturn Booster Operations
Seattle 24, Washington
Attn: R. H. Nelson

North American Aviation
Space and Information Division Systems
12214 Lakewood Boulevard
Downey, California
Attn: A. Shimizu

Chrysler Space Division
Michoud Operations
P. O. Box 26018
New Orleans 26, Louisiana
Attn: V. J. Vehko
B. Heinrich

DISTRIBUTION (CONT.)

EXTERNAL

Scientific and Technical Information Facility (2)
Attn: NASA Representative (S-AK/RKT)
P. O. Box 5700
Bethesda, Maryland